Primordial non-Gaussianity, CMB, LSS, etc. …

Sabino Matarrese
Dipartimento di Fisica "*Galileo Galilei*",
Università degli Studi di Padova, ITALY
email: sabino.matarrese@pd.infn.it

The present view on non-Gaussianity

- Alternative structure formation models of the late eighties considered strongly non-Gaussian primordial fluctuations.
- The increased accuracy in CMB and LSS observations has excluded this extreme possibility.
- The present-day challenge is either detect or constrain mild or weak (~0.1%) deviations from primordial Gaussian initial conditions.
- Deviations of this type are not only possible but are generically predicted in the standard perturbation generating mechanism provided by inflation.

Available online at www.sciencedirect.com
SCIENCE DIRECT®
ELSEVIER
Physics Reports 402 (2004) 103–266
PHYSICS REPORTS
www.elsevier.com/locate/physrep

Non-Gaussianity from inflation: theory and observations

N. Bartolo[a], E. Komatsu[b], S. Matarrese[c, d, *], A. Riotto[d]

[a]*Astronomy Centre, University of Sussex Falmer, Brighton, BN1 9QH, UK*
[b]*Department of Astronomy, The University of Texas at Austin, Austin, TX 78712, USA*
[c]*Dipartimento di Fisica "G. Galilei", Università di Padova, via Marzolo 8, I-35131 Padova, Italy*
[d]*INFN, Sezione di Padova, via Marzolo 8, I-35131 Padova, Italy*

Accepted 9 August 2004
editor: M.P. Kamionkowski

Non-Gaussianity in the initial conditions

Simple-minded NG model

- ✓ Many primordial (inflationary) models of non-Gaussianity can be represented in configuration space by the simple formula (Salopek & Bond 1990; Gangui et al. 1994; Verde et al. 1999; Komatsu & Spergel 2001)

$$\Phi = \phi_L + f_{NL} * (\phi_L^2 - \langle \phi_L^2 \rangle) + g_{NL} * \phi_L^3 + \dots$$

where Φ is the large-scale gravitational potential, ϕ_L its linear Gaussian contribution and f_{NL} is the dimensionless *non-linearity parameter* (or more generally *non-linearity function*). The percent of non-Gaussianity in CMB data implied by this model is

$$\text{NG \%} \sim 10^{-5} |f_{NL}|$$

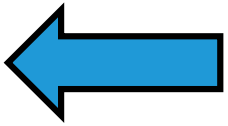

$< 10^{-3}$ from *WMAP*

Where does large-scale non-Gaussianity come from (in standard inflation)?

- *Falk et al. (1993)* found $f_{NL} \sim \xi \sim \varepsilon^2$ (from non-linearity in the inflaton potential in a fixed de Sitter space) in the standard single-field slow-roll scenario

- *Gangui et al. (1994)*, using stochastic inflation found $f_{NL} \sim \varepsilon$ (from second-order gravitational corrections during inflation). *Acquaviva et al. (2003)* and *Maldacena (2003)* confirmed this estimate (up to numerical factors and momentum-dependent terms) with a full second-order approach. Weinberg extended the calculation of the bispectrm to 1-loop …

- *Bartolo et al. (2004, 2005)* showed that second-order corrections after inflation enhance the primordial signal leading to $f_{NL} \sim 1$

Evaluating NG: from inflation to the present universe

- Evaluate non-Gaussianity during inflation by a self-consistent second-order calculation (or equivalent techniques …).
- Evolve scalar (vector) and tensor perturbations to second order after inflation outside the horizon, matching conserved second-order gauge-invariant variable, such as the comoving curvature perturbation $\zeta^{(2)}$ (or non-linear generalizations of it), to its value at the end of inflation (accurately accounting for reheating) or immediately after it.
- Evolve them consistently inside the horizon → compute second-order radiation transfer function for CMB and second-order matter transfer function for DM.
- Large values of $|f_{NL}|$ (>10) still allow us to use the usual first-order radiation transfer function

Summary of NG from inflation

Bartolo, Matarrese & Riotto, 2005; D'Amico, Bartolo, Matarrese & Riotto, 2008

$$\delta T/T = -(\Phi/3)$$

$$\Phi = \Phi_{\rm L} + f_{\rm NL} \star (\Phi_{\rm L})^2 + g_{\rm NL} \star (\Phi_{\rm L})^3,$$

leading contribution to bispectrum:

- Quadratic non-linearity on large-scales (up to ISW and 2-nd order tensor modes). Standard slow-roll inflation yields $a_{NL} \sim b_{NL} \sim 1$

Include SW + ISW up to 3-rd order

$$f_{\rm NL} = -\left[\tfrac{5}{3}(1-a_{\rm NL}) + \tfrac{1}{6}\right] + \left[3(\mathbf{k}_1\cdot\mathbf{k}_3)(\mathbf{k}_2\cdot\mathbf{k}_3)/k^4 - (\mathbf{k}_1\cdot\mathbf{k}_2)/k^2\right]$$

additional contribution to trispectrum (together with f_{NL}^2 terms):

- Cubic non-linearity on large-scales (up to ISW and 2-nd order tensor modes)

$$g_{\rm NL}(\mathbf{k}_1,\mathbf{k}_2,\mathbf{k}_3) = \tfrac{25}{9}(b_{\rm NL}-1) + \tfrac{25}{9}(a_{\rm NL}-1)\mathcal{A}(\mathbf{k}_1,\mathbf{k}_2,\mathbf{k}_3) + \tfrac{25}{9}\mathcal{C}(\mathbf{k}_1,\mathbf{k}_2,\mathbf{k}_3) - \tfrac{5}{9}(a_{\rm NL}-1)$$
$$+ \frac{1}{54} - \frac{1}{3}\left[\frac{(\mathbf{k}_1\cdot(\mathbf{k}_1+\mathbf{k}_2))\,(\mathbf{k}_2\cdot(\mathbf{k}_1+\mathbf{k}_2))}{|\mathbf{k}_1+\mathbf{k}_2|^4} - \frac{1}{3}\frac{\mathbf{k}_1\cdot\mathbf{k}_2}{|\mathbf{k}_1+\mathbf{k}_2|^2} + \text{cycl.}\right],$$

What Inflation predicts

- ✓ Standard single-field slow-roll inflation predicts $a_{NL}-1 \sim 10^{-2}$ (Acquaviva et al. 2001; Maldacena 2001) and similarly tiny values for higher-order parameters, such as $b_{NL}-1$

- ✓ Alternative models (e.g. curvaton, multi-field, inhomogeneous reheating, DBI, ghost inflation, new ekpyrotic, warm-inflation, …) can lead to much higher values for the parameters (functions) $a_{NL}-1$, $b_{NL}-$, etc. …

Inflationary predictions for f_{NL}

Models	$f_{\rm NL}$	Comments
Single–field inflation	$\mathcal{O}(\epsilon,\eta)$	ϵ,η slow-roll parameters
Curvaton scenario	$\frac{5}{4r}-\frac{5}{6}r-\frac{5}{3}$	$r\approx\left(\frac{\rho_\sigma}{\rho}\right)_{decay}$
Inhomogeneous reheating	$-\frac{5}{4}-I$	$I=-\frac{5}{2}+\frac{5}{12}\frac{\Gamma}{\alpha\Gamma_1}$ "minimal case" $I=0$ ($\alpha=\frac{1}{6}$, $\Gamma_1=\bar{\Gamma}$)
Multiple scalar fields	$\frac{\mathcal{P}_\mathcal{S}}{\mathcal{P}_\mathcal{R}}\cos^2\Delta\left(4\cdot10^3\cdot\frac{V_{\chi\chi}}{3H^2}\right)\cdot60\frac{H}{\chi}$	order of magnitude estimate of the absolute value
Warm inflation	$-\frac{5}{6}\left(\frac{\dot{\varphi}_0}{H^2}\right)\left[\ln\left(\frac{\Gamma}{H}\right)\frac{V'''}{\Gamma}\right]$	Γ: inflaton decay rate
Ghost inflation	$-85\cdot\beta\cdot\alpha^{-8/5}$	equilateral configuration
DBI	$-0.2\,\gamma^2$	equilateral configuration
Preheating scenarios	e.g. $\frac{M_{Pl}}{\varphi_0}e^{Nq/2}\sim50$	N: number of inflaton oscillations
Inhomogeneous preheating and inhomogeneous hybrid inflation	e.g. $\frac{5}{6}\lambda_\varphi\left(\frac{M_{Pl}}{m_\chi}\right)^2\sim100$	λ_φ: inflaton coupling to the waterfall field χ
Generalized single-field inflation (including k-inflation and brane inflation)	$-\frac{35}{108}\left(\frac{1}{c_s^2}-1\right)+\frac{5}{81}\left(\frac{1}{c_s^2}-1-2\frac{\lambda}{\Sigma}\right)$	high when the sound speed $c_s\ll1$ or $\lambda/\Sigma\gg1$

Inflationary predictions for f_{NL}

Table 1.2 Predictions for $f_{\rm NL}$ from some unconventional scenarios

Models	$f_{\rm NL}$	Comments
Warm inflation	$-15L(r) < f_{\rm NL} < (33/2)L(r)$	$L(r) \simeq \ln(1 + r/14)$; $r = \frac{\Gamma}{3H} \gg 1$
Generalized slow-roll/ higher-order kin. terms	$f_{\rm NL} \gg +1$	equilateral config.
Excited in. states + interact.	$\sim \left(6.3 \times 10^{-4} \frac{M_P}{M}\right)^5 \sim (1 - 100)$	flatten config. M: cut-off scale
Ekpyrotic models	$-50 \leq f_{\rm NL} \leq +200$	depends on sharpness of conversion from isocurv. to curvature modes.

NG requires higher-order statistics (than power-spectrum or 2-point function)

- The simplest statistics (but not fully general) measuring NG is the 3-point function or its Fourier transform, the "bispectrum":

$$< \delta(\mathbf{k}_1)\delta(\mathbf{k}_2)\delta(\mathbf{k}_3) > = (2\pi)^3\delta^{(3)}(\mathbf{k}_1+\mathbf{k}_2+\mathbf{k}_3)\, B(k_1,k_2,k_3)$$

which also carries shape information

The shape of Non-Gaussianities

Different models for the generation of NG may lead to a different shape dependence of the bispectrum, which is very important for constraining NG

squeezed configurations dominant

equilateral configurations approximately dominant

Babich et al. 2005; Creminelli et al. 2005; LoVerde et al. 2007

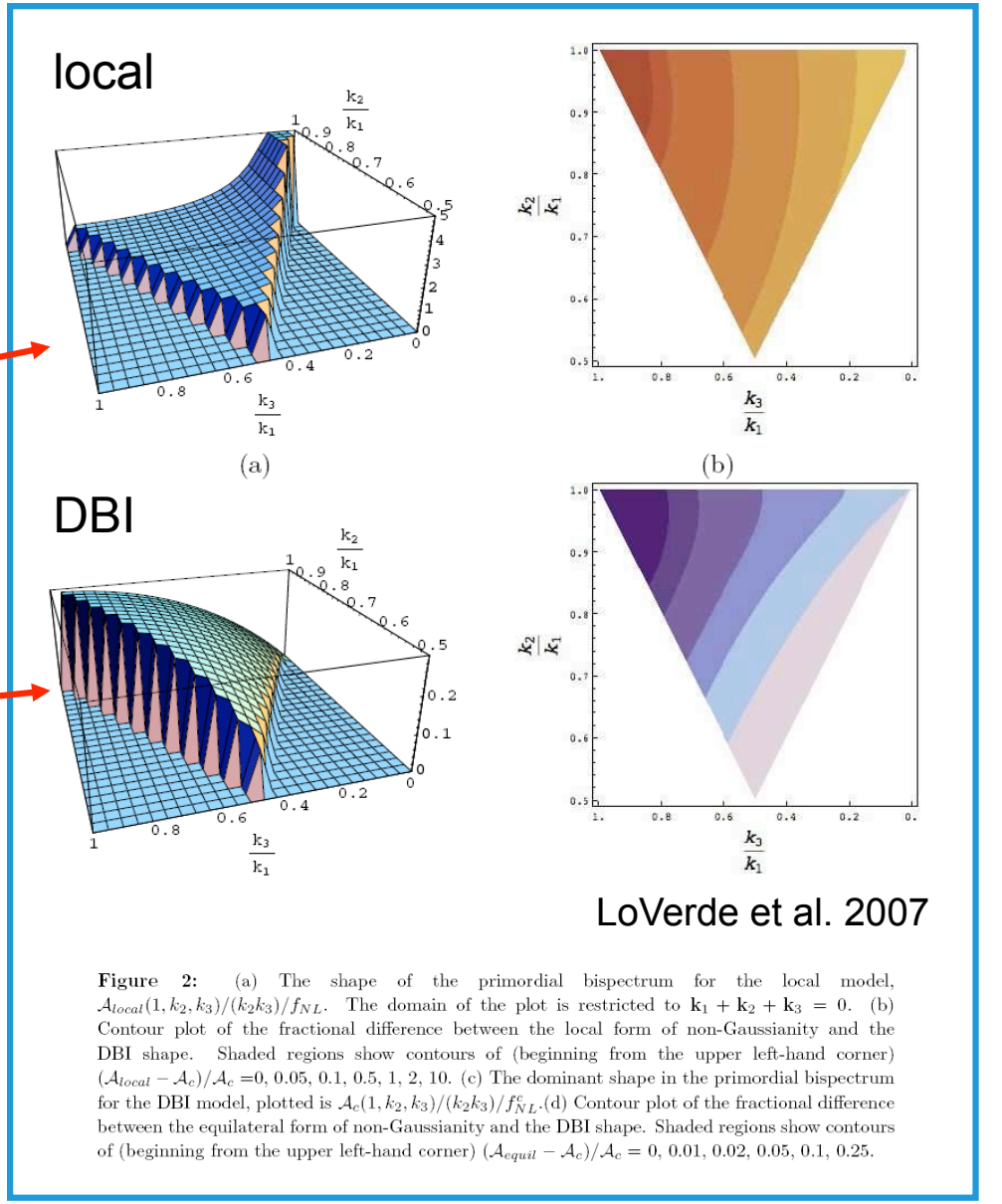

Figure 2: (a) The shape of the primordial bispectrum for the local model, $\mathcal{A}_{local}(1, k_2, k_3)/(k_2 k_3)/f_{NL}$. The domain of the plot is restricted to $\mathbf{k}_1 + \mathbf{k}_2 + \mathbf{k}_3 = 0$. (b) Contour plot of the fractional difference between the local form of non-Gaussianity and the DBI shape. Shaded regions show contours of (beginning from the upper left-hand corner) $(\mathcal{A}_{local} - \mathcal{A}_c)/\mathcal{A}_c$ =0, 0.05, 0.1, 0.5, 1, 2, 10. (c) The dominant shape in the primordial bispectrum for the DBI model, plotted is $\mathcal{A}_c(1, k_2, k_3)/(k_2 k_3)/f^c_{NL}$.(d) Contour plot of the fractional difference between the equilateral form of non-Gaussianity and the DBI shape. Shaded regions show contours of (beginning from the upper left-hand corner) $(\mathcal{A}_{equil} - \mathcal{A}_c)/\mathcal{A}_c$ = 0, 0.01, 0.02, 0.05, 0.1, 0.25.

2-nd order transfer function

- Improve treatment of radiation transfer function.

- This step is crucial for $|f_{NL}| \sim 1$ (i.e. to detect NG from standard single-field sinflation). For large NG (i.e. $|f_{NL}| > \sim 10$) the standard procedure of convolving the NG potential with the linear transfer function is sufficiently accurate.

- This should be O.K. for presently detectable level of NG.

2-nd order transfer function

- First step (Bartolo, Matarrese & Riotto, 2005): calculation of the full 2-nd order radiation transfer function on large scales (low-l), which includes:
  - ✓ NG initial conditions
  - ✓ non-linear evolution of gravitational potentials on large scales
  - ✓ second-order SW effect (and second-order temperature fluctuations on last-scattering surface)
  - ✓ second-order ISW effect, both early and late
  - ✓ ISW from second-order tensor modes (unavoidably arising from non-linear evolution of scalar modes), also accounting for second-order tensor modes produced during inflation

2-nd order transfer function

- ☑ Second step (Bartolo, Matarrese & Riotto, 2006a,b): Boltzmann eq. up to 2-nd order for photon, baryon and CDM fluids allow to follow CMB anisotropies at 2-nd order on all scales; includes both scattering and gravitational secondaries, like:
  - ✓ Thermal and Kinetic Sunyaev-Zel'dovich effect
  - ✓ Ostriker-Vishniac effect
  - ✓ Inhomogeneous recombination and reionization
  - ✓ Further gravitational terms, including gravitational lensing (both by scalar and tensor modes), Rees-Sciama effect, Shapiro time-delay, effects from second-order vector (i.e. rotational) modes, etc.

- ☑ Numerical code shows that the effect is equivalent to an effective f_{NL} ~ few (Nitta, Komatsu, Bartolo, Matarrese & Riotto, 2008, in prep.)

- ☑ Pitrou et al. (2008) have recently obtained large non-linear corrections (~ 25) affecting very small-scale equilateral f_{NL} . These corrections are however not relevant for local NG.

  → see also Serra & Cooray (2008), Cooray et al. (2008).

NG CMB simulated maps

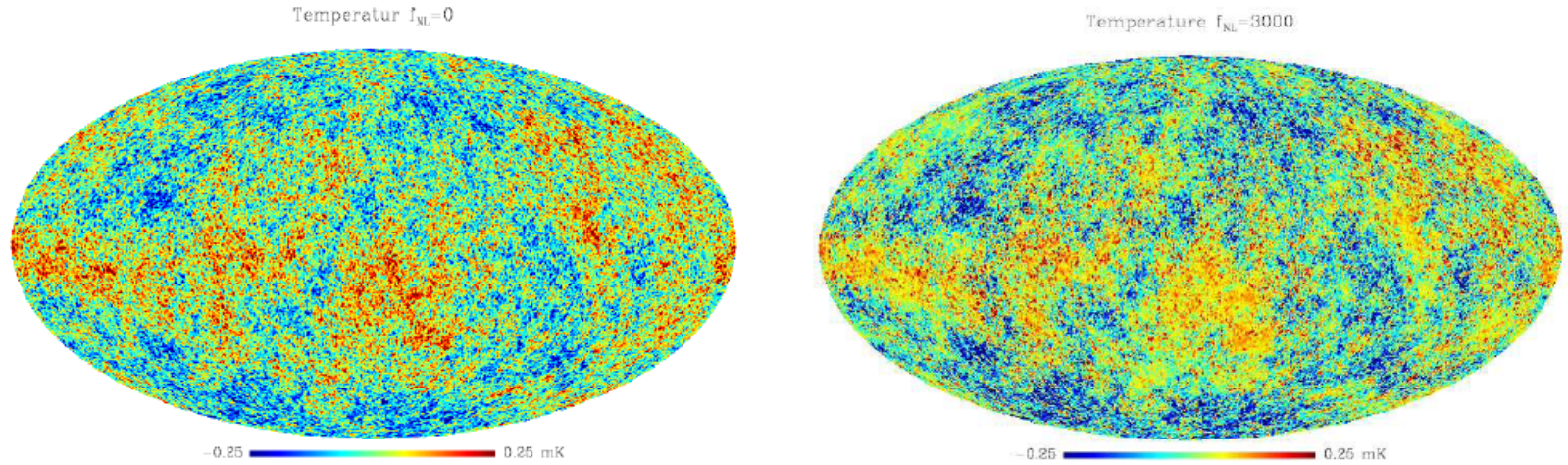

Liguori, Yadav, Hansen, Komatsu, Matarrese & Wandelt 2007

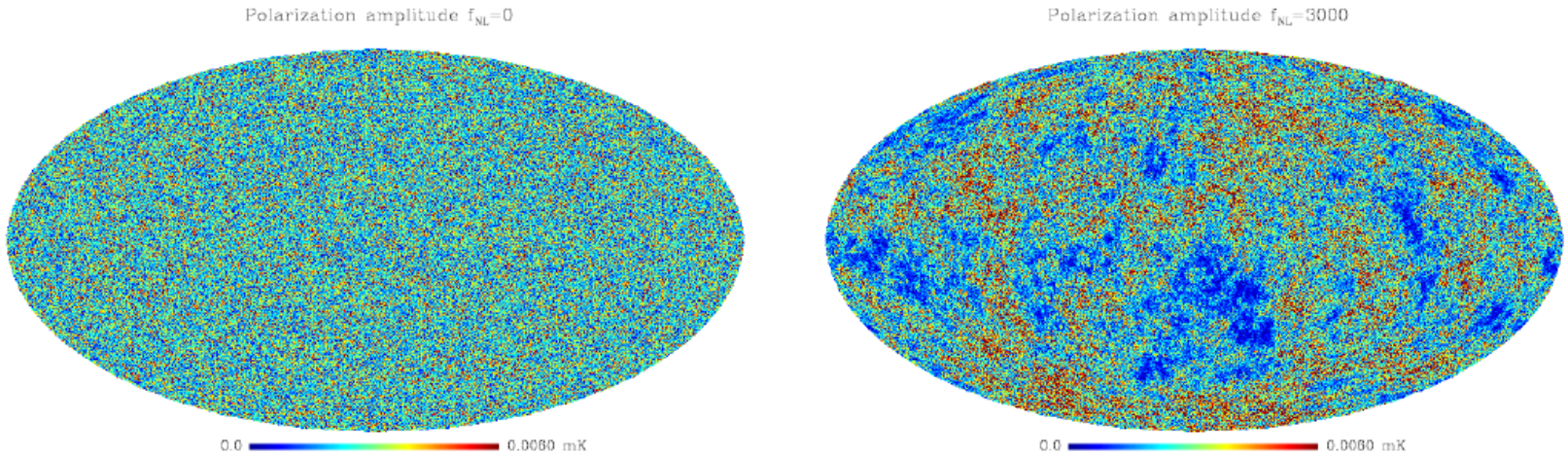

FIG. 8: Left column: temperature and polarization intensity Gaussian CMB simulations obtained from our algorithm. Polarization intensity is defined as $I \equiv \sqrt{Q^2 + U^2}$ where Q and U are the Stokes parameters. Right column: temperature and polarization non-Gaussian maps with the same Gaussian seed as in the left column and $f_{\rm NL} = 3000$. The reason for the choice of such a large $f_{\rm NL}$ is that we wanted to make non-Gaussian effects visible by eye in the figures. The cosmological model adopted for this plots is characterized by: $\Omega_b = 0.042$, $\Omega_{cdm} = 0.239$, $\Omega_L = 0.719$, $h = 0.73$, $n = 1$, $\tau = 0.09$. Temperatures are in mK.

WMAP 5-years constraints on f_{NL}

Komatsu et al. (2008) find

$$-9 < f_{NL}^{\rm local} < 111 \ (95\% \ {\rm CL})$$

(after point-source subtraction) analyzing 5-year WMAP data.

The discrepancy with Yadav & Wandelt (2007) who found positive NG detection in the 3-year WMAP data

$$27 < f_{\rm NL} < 147 \ {\rm at} \ 95\% \ {\rm C.L.}$$

(rejection of f_{NL}=0 at more than 99.5% CL) can be explained in terms of the different mask applied in the analysis and improved resolution of 5-year data.

Curto et al. (2008) find a very similar constraint using wavelets

$$-8 < f_{NL} < 111 \ (95\% \ {\rm CL})$$

Komatsu et al. 2008

TABLE 5
CLEAN-MAP ESTIMATES AND THE CORRESPONDING 68% INTERVALS OF THE LOCAL FORM OF PRIMORDIAL NON-GAUSSIANITY, $f_{NL}^{\rm local}$, THE POINT SOURCE BISPECTRUM AMPLITUDE, b_{src} (IN UNITS OF 10^{-5} $\mu{\rm K}^3$ ${\rm sr}^2$), AND MONTE-CARLO ESTIMATES OF BIAS DUE TO POINT SOURCES, $\Delta f_{NL}^{\rm local}$

Band	Mask	$l_{\rm max}$	$f_{NL}^{\rm local}$	$\Delta f_{NL}^{\rm local}$	b_{src}
V+W	*KQ85*	400	50 ± 29	1 ± 2	0.26 ± 1.5
V+W	*KQ85*	500	61 ± 26	2.5 ± 1.5	0.05 ± 0.50
V+W	*KQ85*	600	68 ± 31	3 ± 2	0.53 ± 0.28
V+W	*KQ85*	700	67 ± 31	3.5 ± 2	0.34 ± 0.20
V+W	*Kp0*	500	61 ± 26	2.5 ± 1.5	
V+W	*KQ75p1*[a]	500	53 ± 28	4 ± 2	
V+W	*KQ75*	400	47 ± 32	3 ± 2	-0.50 ± 1.7
V+W	*KQ75*	500	55 ± 30	4 ± 2	0.15 ± 0.51
V+W	*KQ75*	600	61 ± 36	4 ± 2	0.53 ± 0.30
V+W	*KQ75*	700	58 ± 36	5 ± 2	0.38 ± 0.21

[a]This mask replaces the point-source mask in *KQ75* with the one that does not mask the sources identified in the *WMAP* K-band data

Constraints on non-local NG are much weaker:

$$-151 < f_{NL}^{\rm equil} < 253 \ (95\% \ {\rm CL})$$

Topological constraints on f_{NL}

Hikage, Matsubara, Coles, Liguori, Hansen & Matarrese (2008) find

- $70 < f_{NL} < 91$ at 95% C.L.

using the Q+V+W co-added maps of 3-year WMAP data

Analytical formulae for the Minkowski functionals of NG fields are found in excellent agreement with simulated CMB maps

$$\Delta v_k(\nu, f_{\rm NL}) = e^{-\nu^2/2}\left\{\left[\frac{1}{6}S^{(0)}H_{k+2}(\nu)+\frac{k}{3}S^{(1)}H_k(\nu)\right.\right.$$
$$\left.\left.+\frac{k(k-1)}{6}S^{(2)}H_{k-2}(\nu)\right]\sigma_0+\mathcal{O}(\sigma_0^2)\right\},$$

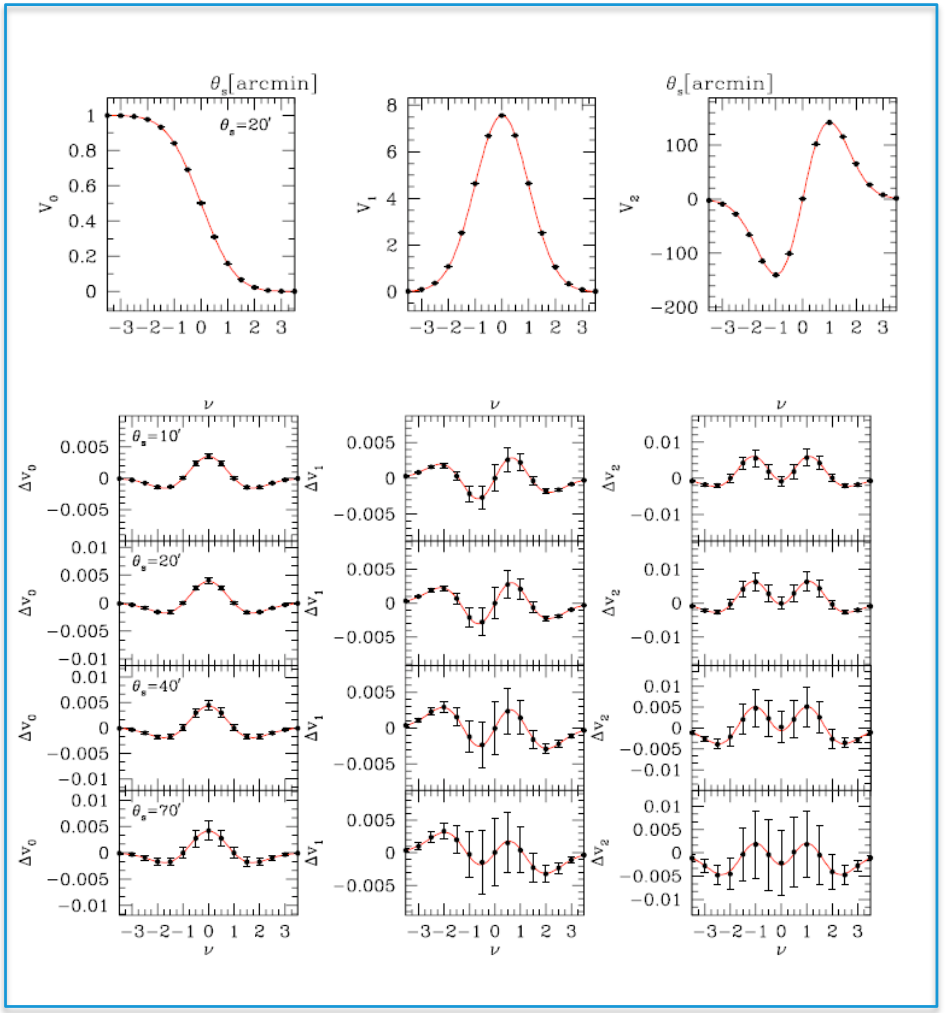

Constraining Non-Standard Inflation with Planck

with Planck:
$\Delta f_{NL}^{equil} \sim 35$

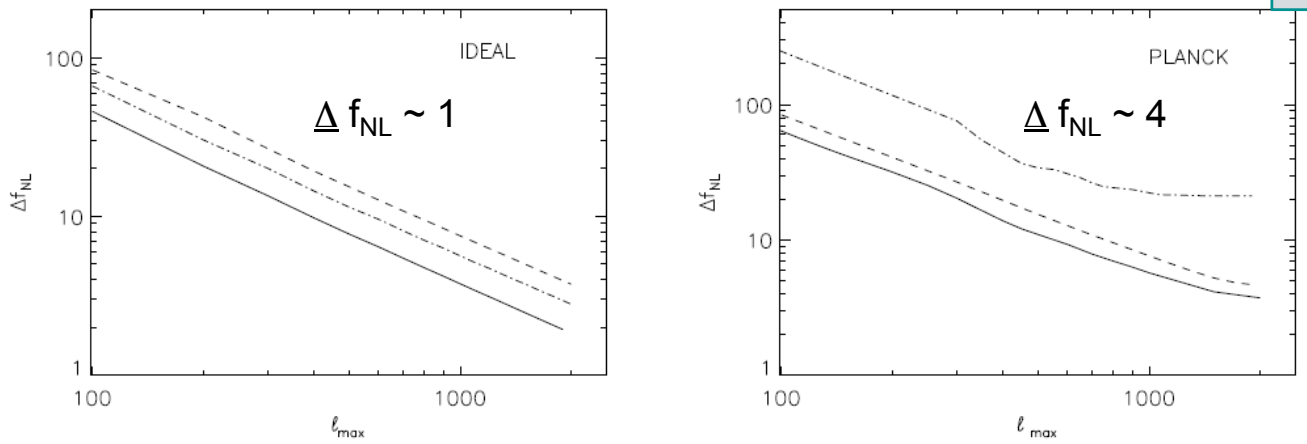

Fig. 2.— Fisher predictions for minimum detectable f_{NL} at the 1-σ level. Left panel: ideal experiment. Right panel: Planck satellite. Solid lines: temperature and polarization information combined. Dashed lines: temperature information only. Dot-dashed line: polarization information only.

Yadav, Komatsu and Wandelt 2007

Searching for NG in Planck data will require accurate handling of residual NG from systematics: work in progress (Donzelli, Hansen, Liguori, Yadav & Matarrese, in prep.)

Fast estimator extended to incomplete sky coverage in Yadav, Komatsu, Wandelt, Liguori, Hansen & Matarrese 2007: see also Creminelli, Nicolis, Senatore & Tegmark 2006

Non-Gaussianity from initial conditions

vs.

non-Gaussianity from gravitational instability

Searching for non-Gaussianity with LSS

- Verde et al. (1999) and Scoccimarro et al. (2004) showed that constraints on primordial NG in the gravitational potential from large redshift-surveys like 2dF and SDSS are not competitive with CMB ones.

- Going to redshift z~2 can make LSS competitive (Sefusatti & Komatsu 2007). Going to higher z, e.g. through SZ cluster surveys, Ly-alpha forest (Viel et al. 2008) or via 21-cm background anisotropies (Pillepich, Porciani & Matarrese 2006; Cooray 2006) helps, as the effective NG strength in the underlying CDM overdensity scales like (1+z).

Need to go beyond standard perturbation theory

- (Linear) perturbation theory proved extremely successful in dealing with CMB data
- The study of the LSS requires better schemes, owing to the crucial role played by the gravitational instability, which makes the underlying dark matter density field unavoidably non-linear, hence non-Gaussian, on a relevant range of scales.
- Renormalized Perturbation Theory (Crocce & Scoccimarro 2005, 2006)
- Renormalization Group (RG) approach (Matarrese & Pietroni 2007; Pietroni 2008)

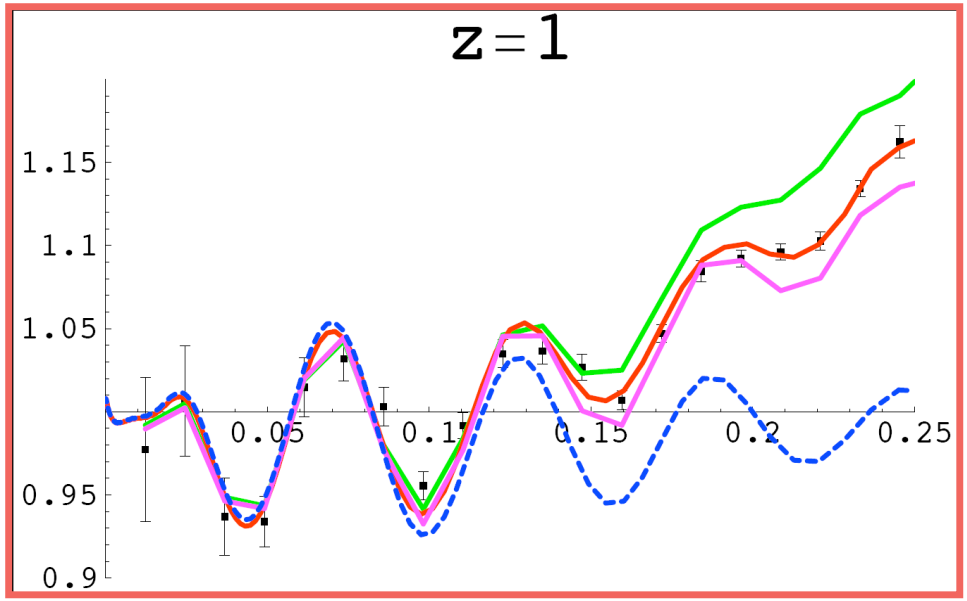

Power-spectrum at z=1as given by RG (red line), linear theory (blue short-dashed), 1-loop PT (green), halo-model (violet) and N-body simulations (squares) by Jeong & Komatsu 2006

RG: short & long-term goals

- Include neutrino contribution (Lesgourgues, Matarrese, Pietroni & Riotto, 2008, in prep.)
- Account for (*statistical*) velocity dispersion, starting from the Vlasov (Klimontovich-Dupree) equation (D'Amico, Matarrese & Pietroni 2008, in prep.). Explains damping of small-scale modes
- Deal with redshift-space distortions and non-linear mass → galaxy bias (Heavens, Matarrese, Pietroni & Verde, in prep.; Matarrese, Pietroni & Porciani, in prep.)
- Extend the method to higher-order: non-linear evaluation of the bispectrum
- Non-linear mapping of density & velocity fields (setting an effective theory)?

N-body simulations of local (constant f_{NL}) NG

M. Grossi, K. Dolag, E. Branchini, S. Matarrese & L. Moscardini 2007

- ✓ Standard CDM "concordance" model with: **Ω_{m0}=0.3, $\Omega_{\Lambda 0}$=0.7, h=0.7, σ_8=0.9, n=1**
- ✓ 9 models with: **f_{NL} = -2000, -1000, -500, -100, 0, +100, +500, +1000, +2000**
- ✓ **800^3 particles,** corresponding to a mass-resolution of $m_p \approx 2 * 10^{10}$ solar masses
- ✓ Cosmological boxes: **$L=500^3$ $(Mpc/h)^3$**
- ✓ Computations performed at *CINECA Supercomputing Centre* (Bologna) on a3k (only initial conditions) and sp5 machines: about 3000/5000 hours of CPU time per simulation. A second set of simulations has run at MPA (Garching).

→ see also recent related work by Dalal et al. 2007

The smoothed density field

NG initial conditions:

$$\Phi = \Phi_L + f_{NL}(\Phi_L^2 - \langle \Phi_L^2 \rangle)$$

$$\nabla^2(\Phi * T)g(z) = -4\pi G a^2 \delta\rho_{DM}$$

growth suppression factor

matter transfer function

Hikage, Coles, Grossi, Moscardini, Dolag, Branchini & Matarrese 2007

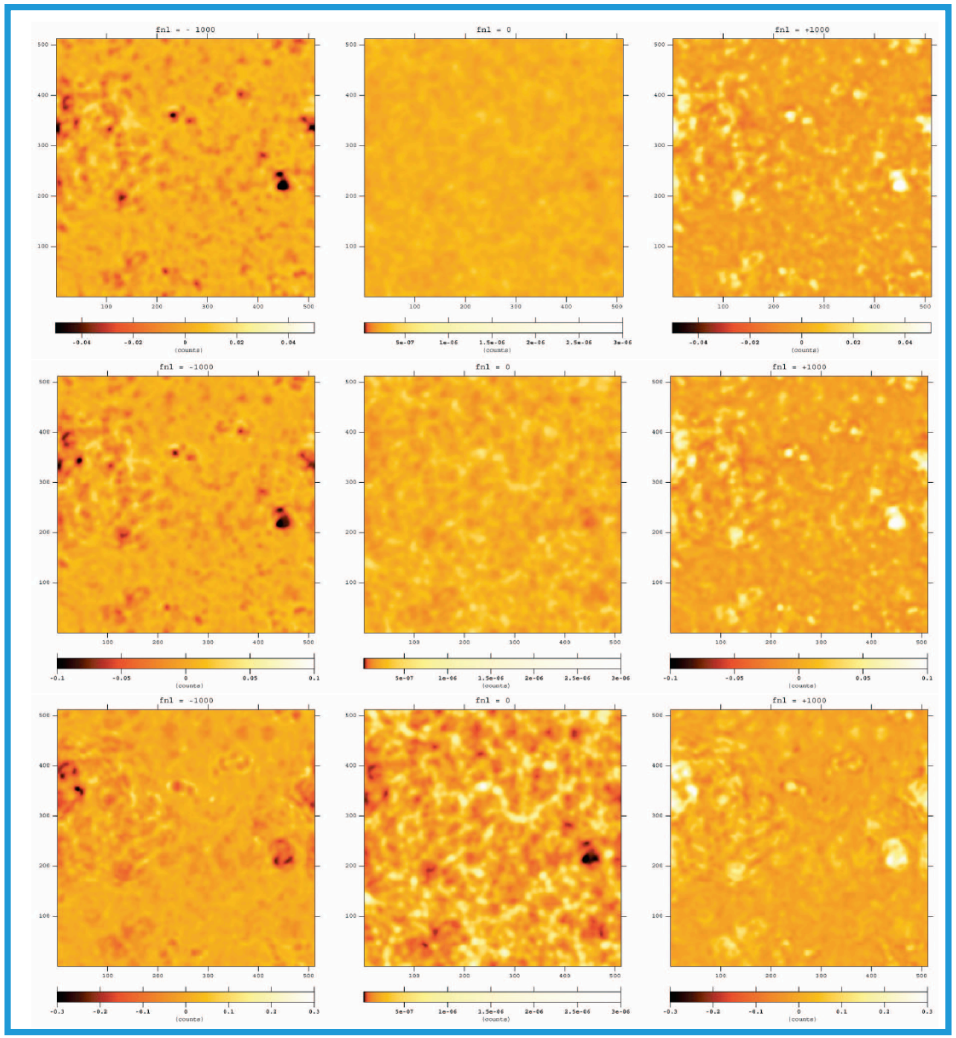

Figure 1. Slice maps of simulated mass density fields at $z = 5.15$ (*top*), $z = 2.13$ (*middle*) and $z = 0$ (*bottom*). The number of pixels at a side length is 512 ($500h^{-1}$Mpc) and that of the thickness is 32 ($31.25h^{-1}$Mpc). The panels in the middle row show the log of the projected density smoothed with a Gaussian filter of 10 pixels width, corresponding to $9.8h^{-1}$Mpc. The left and right panels are the relative residuals for the $f_{\rm NL}=\pm1000$ runs (equation [17]). Each panel has the corresponding color bar and the range considered are different from panel to panel.

Topological measures of NG

Hikage, Coles, Grossi, Moscardini, Dolag, Branchini & Matarrese 2007

Analytical formulae for the Minkowski functionals of non-linearly evolved NG fields are found in excellent agreement with N-body simulations

Indirect check on statistical validity of N-body simulations

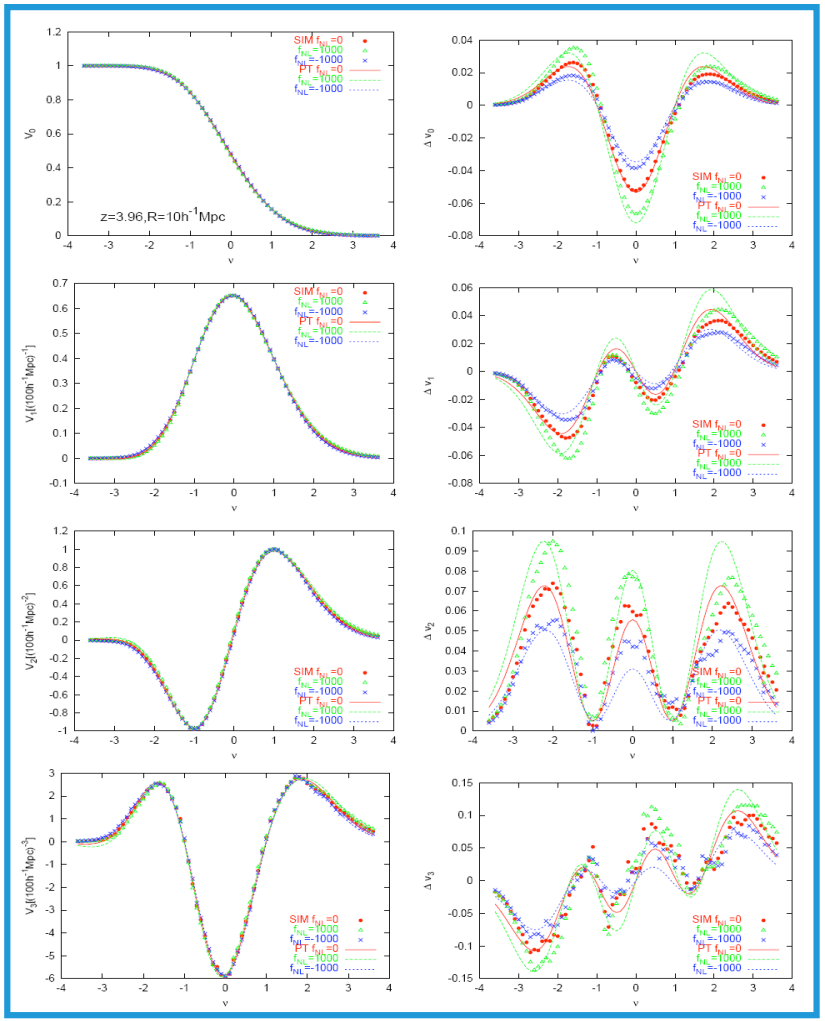

Figure 2. Four Minkowski Functionals V_k (*left*) and their difference ratios Δv_k (*right*) for the simulated mass density fields at $z = 3.96$, with $f_{\rm NL} = 0$ (filled circles), 1000 (open triangles) and -1000 (crosses). The simulated fields are smoothed with a Gaussian window function at the scale of $10h^{-1}$Mpc. For comparison, the theoretical expectations from perturbation theory (equations [2] and [7]) are plotted with lines.

Evolution of the PDF in NG models

Grossi et al. 2008

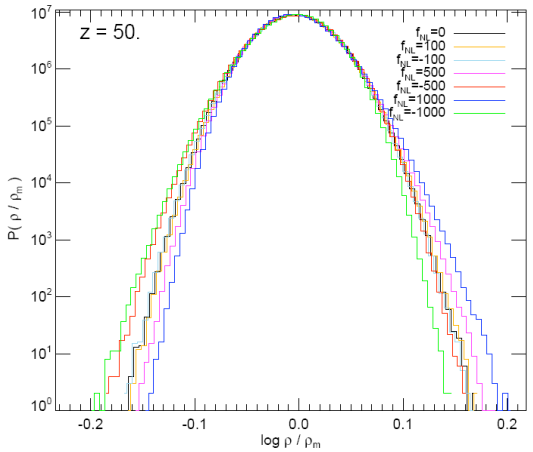

Figure 1. The probability density distribution for the different models (as indicated in the plot) as computed at the earliest common redshift ($z = 50$).

early times: primordial NG affects both low- and high-density tails

late times: primordial NG still affects low-density tails

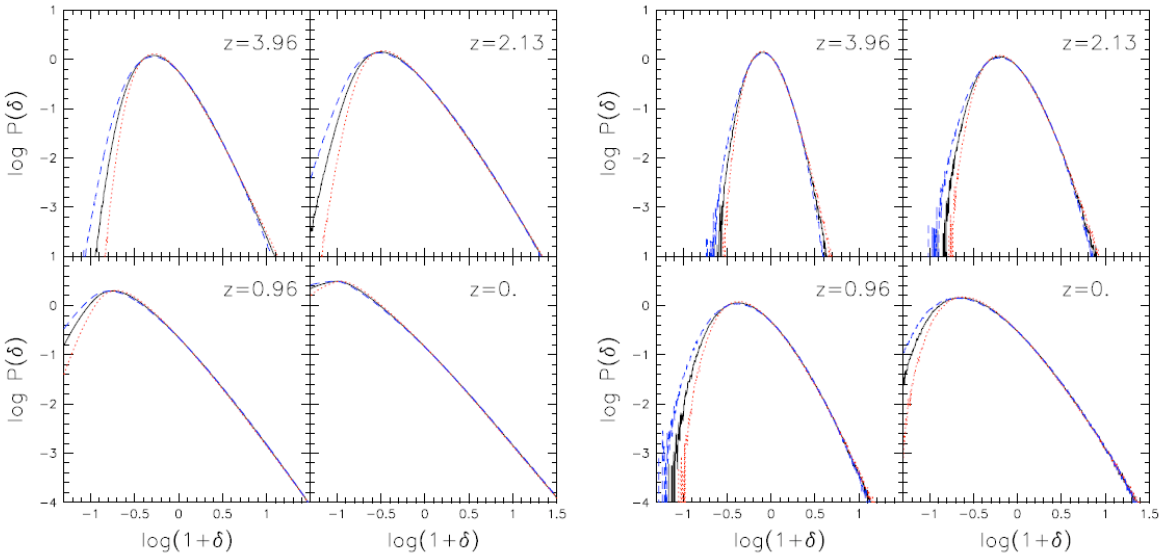

Figure 5. The redshift evolution of the PDF of the density field smoothed on two different scales. Panels on the left: smoothing radius $R_s \sim 0.98$ Mpc/h. Panels on the right: smoothing radius $R_s \sim 3.91$ Mpc/h. The different panels refer to the four redshifts explored, indicated in the plots. Different line-styles refer to models with different primordial non-Gaussianity: $f_{\rm NL} = 0$ (solid line), $f_{\rm NL} = 1000$ (dotted line), $f_{\rm NL} = -1000$ (dashed line).

Fitting NG with log-normal PDF

robust void statistics needed!

Grossi et al. 2008

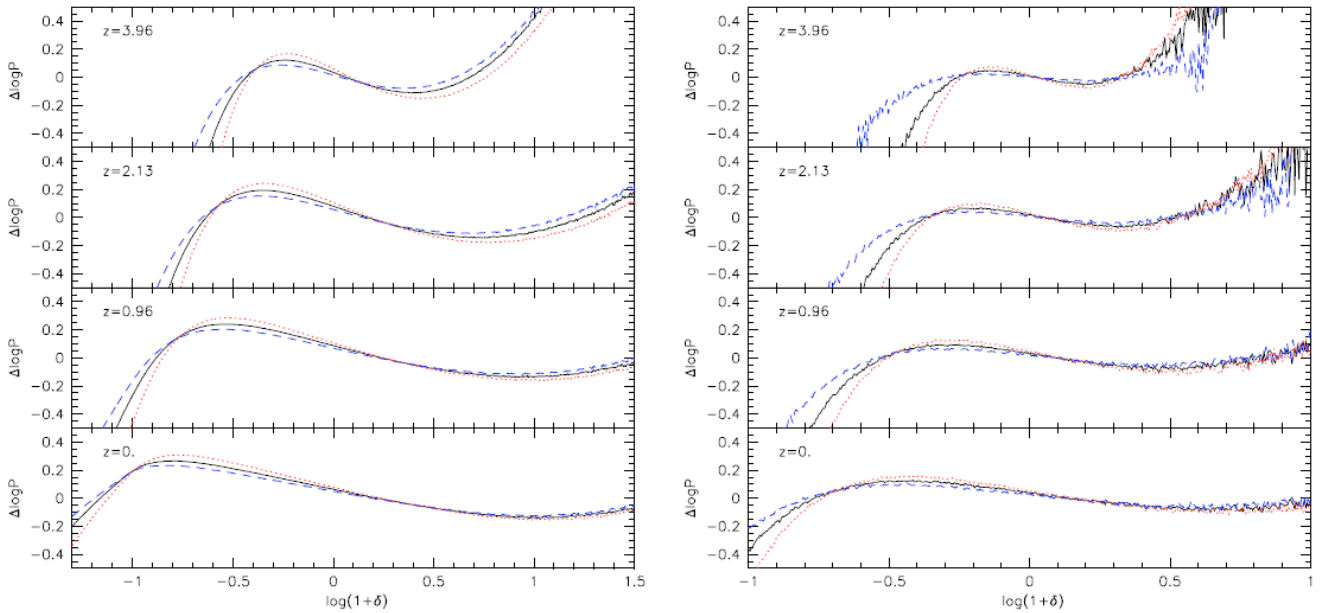

Figure 6. The logarithmic deviation of PDF from a lognormal distribution, $\Delta \log P$, is shown for the same models and redshifts presented in Fig. 5. Results for smoothing radii of $R_s \sim 0.98$ and $R_s \sim 3.91$ Mpc/h are displayed in left and right panels, respectively. Different lines refer to models with different primordial non-Gaussianity: $f_{\rm NL} = 0$ (solid line), $f_{\rm NL} = 1000$ (dotted line), $f_{\rm NL} = -1000$ (dashed line).

Searching for non-Gaussianity with rare events

- Besides using standard statistical estimators, like bispectrum, trispectrum, three and four-point function, skewness , etc. …, one can look at the tails of the distribution, i.e. at rare events.
- Rare events have the advantage that they often maximize deviations from what predicted by a Gaussian distribution, but have the obvious disadvantage of being rare! But remember that, according to Press-Schechter-like schemes, all collapsed DM halos correspond to (rare) peaks of the underlying density field.
- Matarrese, Verde & Jimenez (2000) and Verde, Jimenez, Kamionkowski & Matarrese showed that clusters at high redshift (z>1) can probe NG down to $f_{NL} \sim 10^2$ which is, however, not competitive with future CMB (Planck) constraints.
- Determination of mass function using stochastic approach (first-crossing probability) in progress (Bartolo, Maggiore, Matarrese & Riotto, 2008 in prep.)

Table 1. Minimum $|\epsilon_A|$ and $|\epsilon_B|$ detectable form different observables and their sign when positive skewness is required for detection. For Model A the primordial skewness has the same sign as ϵ_A, while for Model B the primordial skewness has the opposite sign as ϵ_B. In detecting non-zero $\epsilon_{A,B}$ from CMB maps, the sign of the skewness does not influence the accuracy of the detection of non-Gaussianity, but, when using the abundance of high-redshift objects it is robust to detect non-Gaussianity that produces an excess rather than a defect in the number density. Only a positively skewed primordial distribution will generate more high-redshift objects than predicted in the Gaussian case.

Observable	Min. $\lvert\epsilon_A\rvert$	Min. $\lvert\epsilon_B\rvert$
CMB	$10^{-3} \sim 10^{-2}$	20
LSS	10^{-2}	$10^3 \sim 10^4$
High-z obj.	$(+)5 \times 10^{-4}$ (gal.)	$(-)$ 200 (clusters)
ST relation	$(+)3 \times 10^{-3}$	$(-)$ 500

DM halos in NG simulations

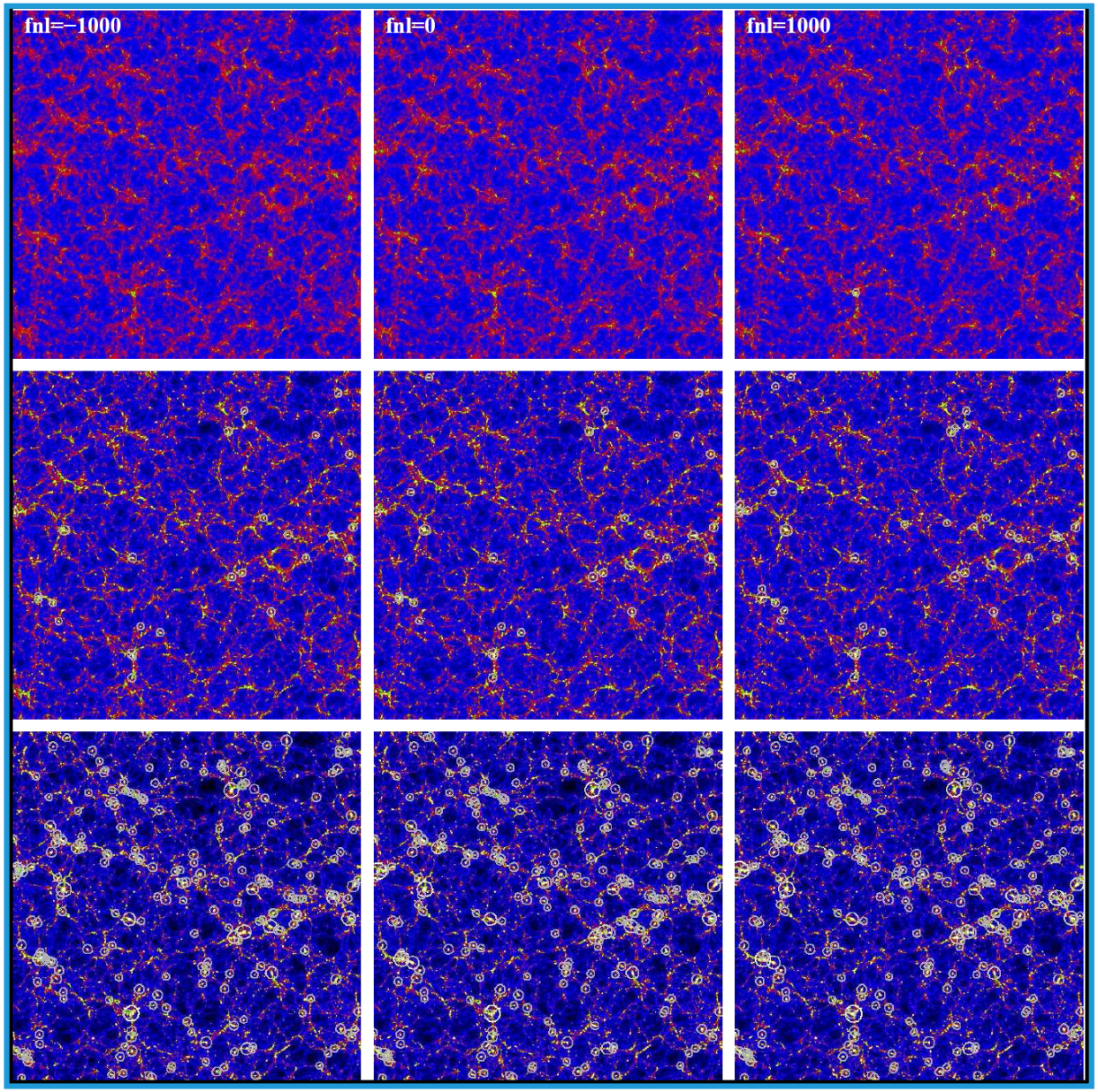

from:
Grossi et al. 2008

DM halo mass-function in NG models

Deviations from the Gaussian mass-function in excellent agreement with the theoretical predictions by Matarrese, Verde & Jimenez (2000):

$$F_{NG}(M, z, f_{\rm NL}) \simeq \frac{1}{6}\frac{\delta_c^2(z_c)}{\delta_*(z_c)}\frac{dS_{3,M}}{d\ln\sigma_M} + \frac{\delta_*(z_c)}{\delta_c(z_c)}$$

where F_{NG} represents the NG/G mass-function ratio

$$n(M, z, f_{\rm NL}) = n_G(M, z)\, F_{NG}(M, z, f_{\rm NL})$$

and

$$\delta_*(z_c) = \delta_c(z_c)\sqrt{1 - S_{3,M}\delta_c(z_c)/3},$$

with $S_{3,M}$ the skewness of the mass-density field on scale M

$$S_{3,M} \equiv \frac{\langle\delta_M^3\rangle}{\sigma_M^4} \propto -f_{\rm NL}$$

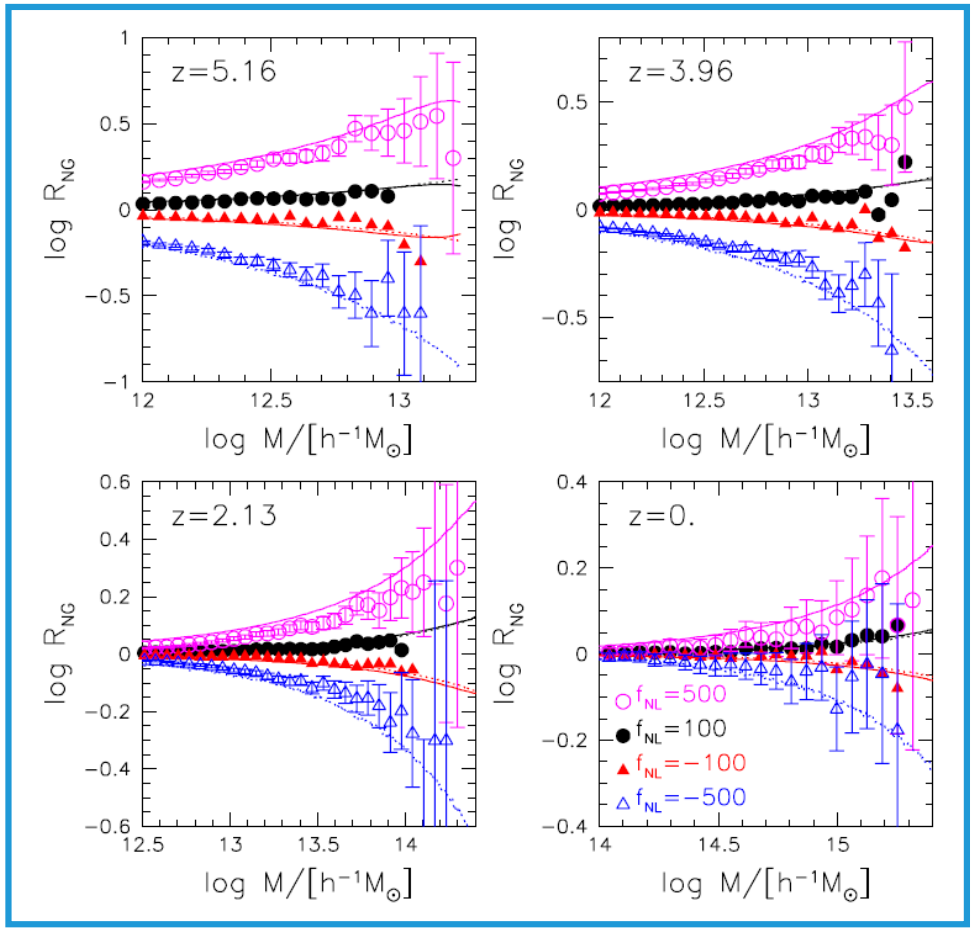

Grossi et al. 2007

Figure 3. Logarithm of the ratio of the halo cumulative mass functions R_{NG} as a function of the mass is shown in the different panels at the same redshifts as in Fig. 1. Circles and triangles refer to positive and negative values for $f_{\rm NL}$; open and filled symbols refer to $f_{\rm NL} = \pm 500$ and $f_{\rm NL} = \pm 100$, respectively. Theoretical predictions obtained starting from eqs. (3) and (4) are shown by dotted and solid lines, respectively. Poisson errors are shown for clarity only for the cases $f_{\rm NL} = \pm 500$.

DM halo bias as a constraint on NG

Dalal et al. (2007) have shown that halo bias is sensitive to primordial non-Gaussianity
through a scale-dependent correction term

$$\Delta b(k)/b \;\alpha\; 2\, f_{NL}\delta_c / k^2$$

This opens interesting prospects for constraining or measuring NG in LSS but demands for an accurate evaluation of the effects of (general) NG on halo biasing.

Dalal, Dore', Huterer & Shirokov 2007

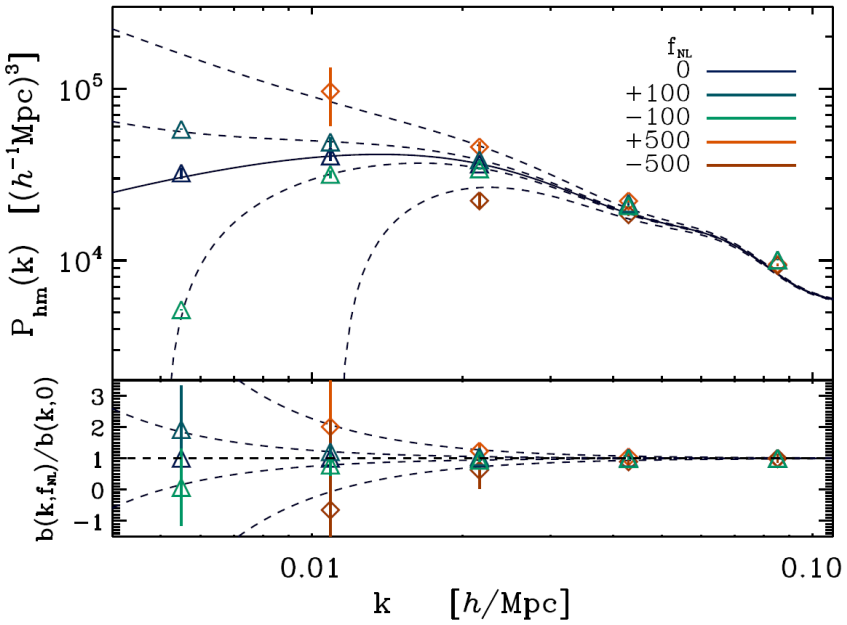

Clustering of peaks (DM halos) of NG density field

Start from results obtained in the 80's by

Grinstein & Wise 1986, ApJ, 310, 19

Matarrese, Lucchin & Bonometto 1986, ApJ, 310, L21

giving the general expression for the peak 2-point function as a function of N-point connected correlation functions of the background linear (i.e. Lagrangian) mass-density field

$$\xi_{h,M}(|\mathbf{x}_1 - \mathbf{x}_2|) = -1 + \exp\left\{ \sum_{N=2}^{\infty} \sum_{j=1}^{N-1} \frac{\nu^N \sigma_R^{-N}}{j!(N-1)!} \xi^{(N)} \begin{bmatrix} \mathbf{x}_1,\ldots,\mathbf{x}_1, & \mathbf{x}_2,\ldots\ldots,\mathbf{x}_2 \\ j\,times & (N-j)\,times \end{bmatrix} \right\}$$

(requires use of path-integral, cluster expansion, multinomial theorem and asymptotic expansion). The analysis of NG models was motivated by a paper by Vittorio, Juszkiewicz and Davis (1986) on bulk flows.

THE ASTROPHYSICAL JOURNAL, 310:L21–L26, 1986 November 1

A PATH-INTEGRAL APPROACH TO LARGE-SCALE MATTER DISTRIBUTION ORIGINATED BY NON-GAUSSIAN FLUCTUATIONS

SABINO MATARRESE
International School for Advanced Studies, Trieste, Italy
FRANCESCO LUCCHIN
Dipartimento di Fisica G. Galilei, Padova, Italy
AND
SILVIO A. BONOMETTO
International School for Advanced Studies, Trieste, Italy; Dipartimento di Fisica G. Galilei, Padova, Italy; and INFN, Sezione di Padova
Received 1986 July 7; accepted 1986 August 1

ABSTRACT

The possibility that, in the framework of a biased theory of galaxy clustering, the underlying matter distribution be non-Gaussian itself, because of the very mechanisms generating its present status, is explored. We show that a number of contradictory results, seemingly present in large-scale data, in principle can recover full coherence, once the requirement that the underlying matter distribution be Gaussian is dropped. For example, in the present framework the requirement that the two-point correlation functions vanish at the same scale (for different kinds of objects) is overcome. A general formula, showing the effects of a non-Gaussian background on the expression of three-point correlations in terms of two-point correlations, is given.

Subject heading: galaxies: clustering

THE ASTROPHYSICAL JOURNAL, 310:19–22, 1986 November 1

NON-GAUSSIAN FLUCTUATIONS AND THE CORRELATIONS OF GALAXIES OR RICH CLUSTERS OF GALAXIES[1]

BENJAMIN GRINSTEIN[2] AND MARK B. WISE[3]
California Institute of Technology
Received 1986 March 6; accepted 1986 April 18

ABSTRACT

Natural primordial mass density fluctuations are those for which the probability distribution, for mass density fluctuations averaged over the horizon volume, is independent of time. This criterion determines that the two-point correlation of mass density fluctuations has a Zeldovich power spectrum (i.e., a power spectrum proportional to k at small wavenumbers) but allows for many types of reduced (connected) higher correlations. Assuming galaxies or rich clusters of galaxies arise wherever suitably averaged natural mass density fluctuations are unusually large, we show that the two-point correlation of galaxies or rich clusters of galaxies can have significantly more power at small wavenumbers (e.g., a power spectrum proportional to $1/k$ at small wavenumbers) than the Zeldovich spectrum. This behavior is caused by the non-Gaussian part of the probability distribution for the primordial mass density fluctuations.

Subject headings: cosmology — galaxies: clustering

Halo bias in NG models

- Matarrese & Verde 2008 have applied this relation to the case of local NG of the gravitational potential, obtaining the power-spectrum of dark matter halos modeled as high “peaks” (upcrossing regions) of height $\nu=\delta_c/\sigma_R$ of the underlying mass density field (Kaiser’s model). Here $\delta_c(z)$ is the critical overdensity for collapse (at redshift a) and σ_R is the *rms* mass fluctuation on scale R ($M \sim R^3$)

- Next, account for motion of peaks (going from Lagrangian to Eulerian space), which implies (Catelan et al. 1998)

$$1+\delta_h(\mathbf{x}_{Eulerian})=(1+\delta_h(\mathbf{x}_{Lagrangian}))(1+\delta_R(\mathbf{x}_{Eulerian}))$$

  and (to linear order) $b=1+b_L$ (Mo & White 1996) to get the scale-dependent halo bias in the presence of NG initial conditions.

- Similar formulae apply to the correlation of CMB hot & cold spots (Heavens, Liguori, Matarrese & Verde, in prep.)

Halo bias in NG models

Matarrese & Verde 2008

$$b_{\rm h}^{f_{\rm NL}} = 1 + \frac{\Delta_c(z)}{\sigma_R^2 D^2(z)} \left[1 + 2 f_{\rm NL} \frac{\Delta_c(z)}{D(z)} \frac{\mathcal{F}_R(k)}{\mathcal{M}_R(k)} \right]$$

form factor:

$$\mathcal{F}_R(k) = \frac{1}{8\pi^2 \sigma_R^2} \int dk_1 k_1^2 \mathcal{M}_R(k_1) P_\phi(k_1) \times \int_{-1}^{1} d\mu \mathcal{M}_R\left(\sqrt{\alpha}\right) \left[\frac{P_\phi\left(\sqrt{\alpha}\right)}{P_\phi(k)} + 2 \right]$$

$$\alpha = k_1^2 + k^2 + 2 k_1 k \mu$$

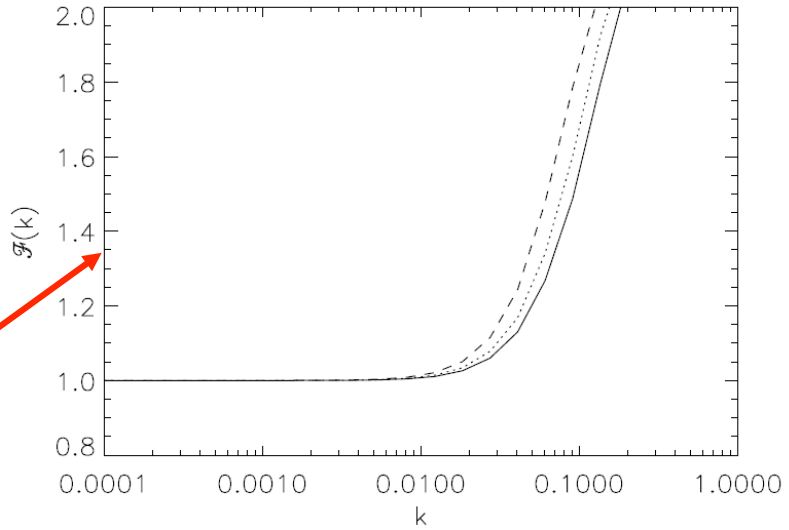

FIG. 1.— The function $\mathcal{F}_R(k)$ for three different masses: 1×10^{14} $M_\odot$ (solid), 2×10^{14} $M_\odot$ (dotted), 1×10^{15} $M_\odot$ (dashed).

factor connecting the smoothed linear overdensity with the primordial potential:

power-spectrum of a Gaussian gravitational potential

$$\mathcal{M}_R(k) = \frac{2}{3} \frac{T(k) k^2}{H_0^2 \Omega_{m,0}} W_R(k)$$

transfer function:

window function defining the radius R of a proto-halo of mass M(R):

Halo bias in NG models

- The NG correction to the halo bias is scale, mass and redshift dependent

- Neglecting the effect of the form factor $F_R(k)$, of the transfer function T(k) and of the window function $W_R(k)$ leads to an error of up to 100% in the NG bias correction and hence in f_{NL}

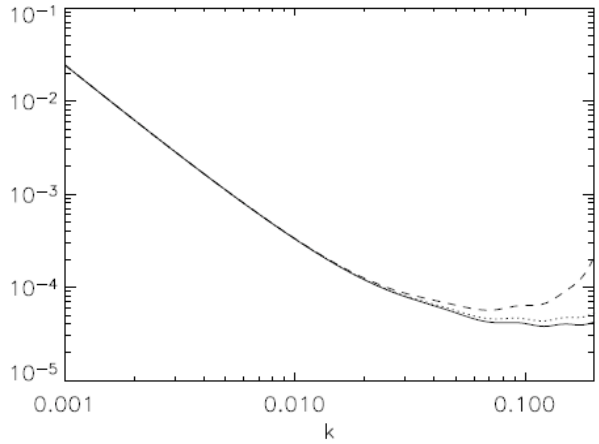

FIG. 3.— The scale dependence of $\Delta b_h/b_h$ for three different masses: 1×10^{14} $M_\odot$ (solid), 2×10^{14} $M_\odot$ (dotted), 1×10^{15} $M_\odot$ (dashed).

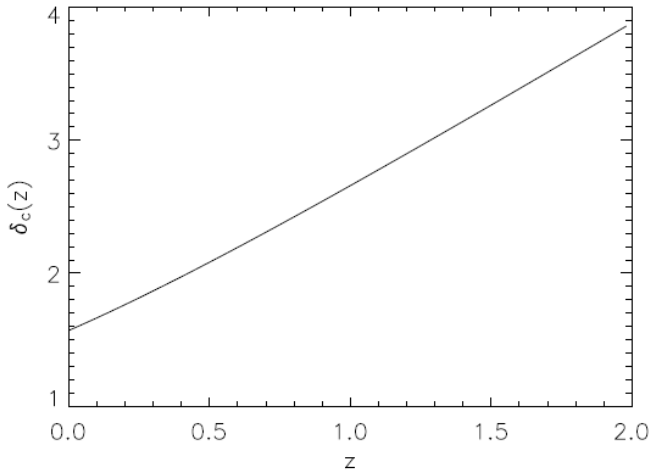

FIG. 2.— The redshift dependence of $\Delta b_h/b_h$.

Halo bias in NG models

- Extension to general (scale and configuration dependent) NG is straightforward

- In full generality write the ϕ bispectrum as $B_\phi(k_1,k_2,k_3)$. The relative NG correction to the halo bias is

$$\frac{\Delta b_h}{b_h} = \frac{\Delta_c(z)}{D(z)} \frac{1}{8\pi^2\sigma_R^2} \int dk_1 k_1^2 \mathcal{M}_R(k_1) \times \int_{-1}^{1} d\mu \mathcal{M}_R\left(\sqrt{\alpha}\right) \frac{B_\phi(k_1, \sqrt{\alpha}, k)}{P_\phi(k)}$$

$$\alpha = k_1^2 + k^2 + 2k_1 k\mu$$

- It also applies to non-local (e.g. “equilateral”) NG (DBI, ghost inflation, etc..)!!

Theory vs. N-body simulations

Grossi, Verde, Branchini, Carbone, Dolag, Matarrese & Moscardini 2008

L_{box} = 1200 Mpc/h, 800^3 particles
Ω_m = 0.26, Ω_Λ = 0.74, H_0 = 0.72
σ_8 = 0.8, n_s = 0.96
softening length 25 kpc, M_{dm} = 1.41 x 10^{11} M_{sun}/h

Our)preliminary) results show that the Matarrese & Verde bias formula provides a very good fit of the bias of DM halos in NG N-body simulations

$$\Delta b = 2q' f_{NL} \delta_c (b_h^G - 1) \alpha(k) .$$

For the Gaussian halo bias b^G, use e.g. Sheth & Tormen (2000)

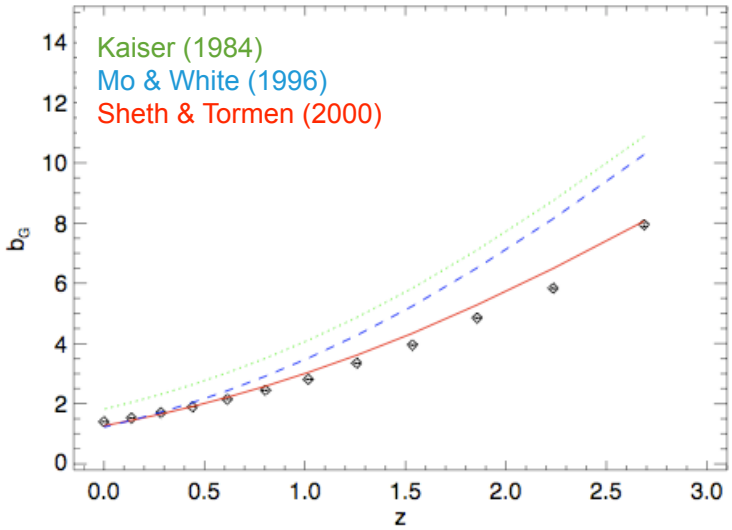

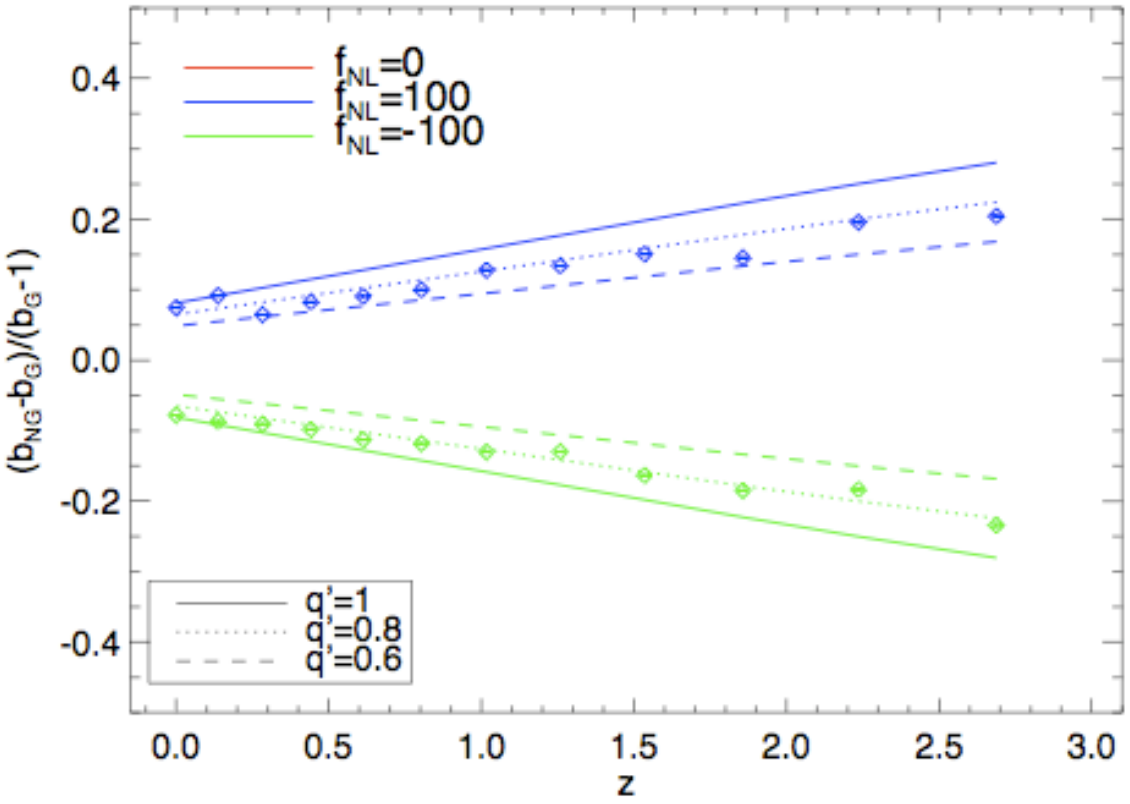

Constraints on f_{NL} from SDSS

SDSS LRG & QSO auto-correlation + WMAP yields:
-1 (-23) < f_{NL} < +70 (+86) @ 95 (99.7) %

Slosar, Hirata, Seljak, Ho & Padmanabhan (2008)

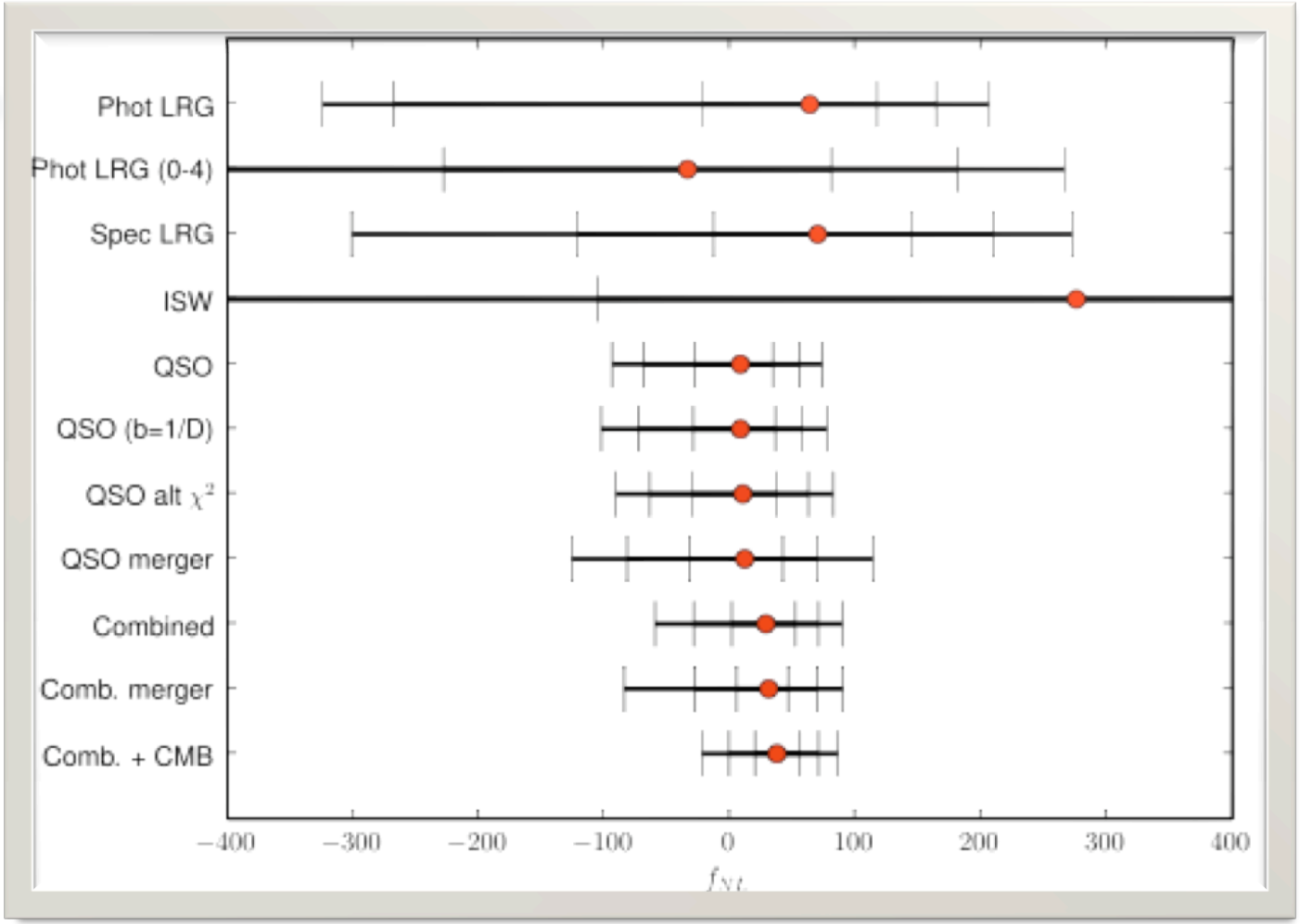

Detecting primordial NG with (ISW driven) LSS-CMB cross-correlation?

WMAP-LSS (NVSS) cross-correlation: LCDM fits the data, once b(z) and N(z) are consistently chosen (e.g. they should also fit auto-correlation function w(θ) !!)

from: Raccanelli, Bonaldi, Negrello, Matarrese, Tormen & De Zotti (2008)

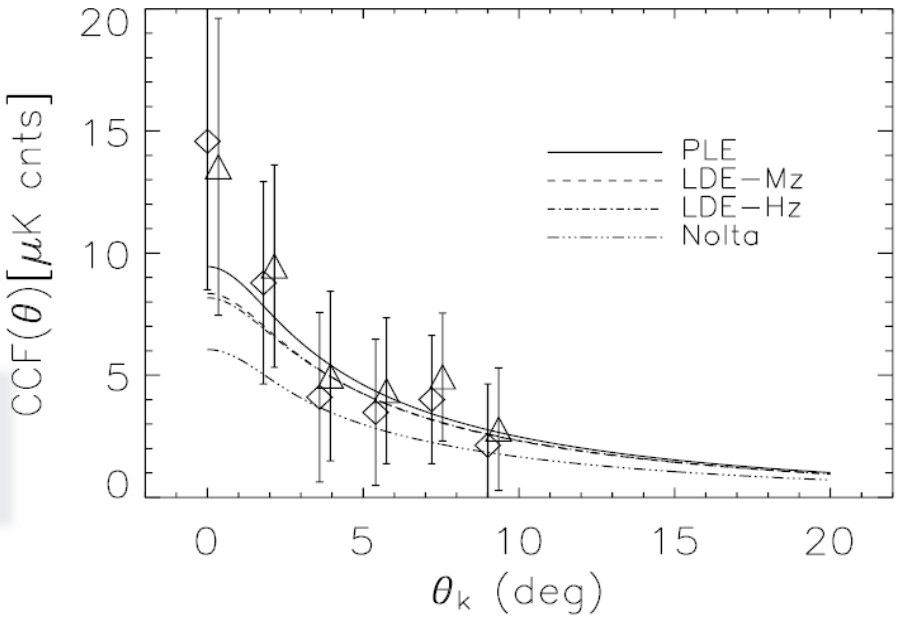

A study of NG detectability, based on large-size, high-mass resolution N-body simulations with NG initial conditions is in progress → Carbone, Branchini, Dolag, Grossi, Matarrese, Moscardini & Verde 2008, in preparation

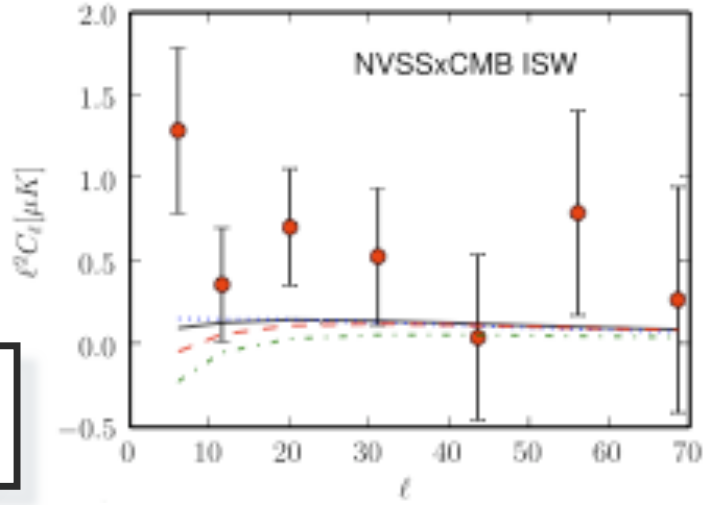

from: Slosar, Hirata, Seljak, Ho & Padmanabhan (2008)

Forecasting constraints on f_{NL} from galaxy surveys

- Carbone, Verde & Matarrese (2008) have obtained (Fisher matrix) forecast of the minimum f_{NL} detectable from galaxy surveys via auto-correlation analyses both projected and in z-space. The minimum detectable f_{NL} is of order a few for future surveys over volume comparable to the Hubble volume. LSS-CMB cross-correlation (via ISW) is also a a promising, though less powerful, technique. See also Afshordi 2008, McDonald 2008, Slosar et al. 2008, Seljak 2008.
- For such low values of NG the scale and shape-dependence of f_{NL} implied by super-horizon evolution (Bartolo, Matarrese & Riotto 2004) of perturbations cannot be disregarded as usually done!
- Related calculations in: Slosar et al. 2008, Afshordi & Tolley 2008, McDonald 2008, Seljak 2008.

Forecasting constraints on f_{NL} from galaxy surveys

Carbone, Verde and Matarrese 2008

$\alpha \sim 1/k^2$ only on the largest scales

error in determination of (local) f_{NL}

$$\frac{1}{\sigma^2_{f_{\rm NL}}} = \frac{8}{2\pi^2}\frac{\Delta_c(z)^2}{D(z)^2} V_{eff} \int_{k_{min}}^{k_{max}} \alpha(k)^2 k^2 dk$$

survey	z range	sq deg	mean galaxy density $(h/Mpc)^3$	$\Delta f_{\rm NL}/q'$ LSS
SDSS LRG's	$0.16 < z < 0.47$	7.6×10^3	1.36×10^{-4}	40
BOSS	$0 < z < 0.7$	10^4	2.66×10^{-4}	18
WFMOS low z	$0.5 < z < 1.3$	2×10^3	4.88×10^{-4}	15
WFMOS high z	$2.3 < z < 3.3$	3×10^2	4.55×10^{-4}	17
ADEPT	$1 < z < 2$	2.8×10^4	9.37×10^{-4}	1.5
EUCLID	$0 < z < 2$	2×10^4	1.56×10^{-3}	1.7
DES	$0.2 < z < 1.3$	5×10^3	1.85×10^{-3}	8
PanSTARRS	$0 < z < 1.2$	3×10^4	1.72×10^{-3}	3.5
LSST	$0.3 < z < 3.6$	3×10^4	2.77×10^{-3}	0.7

Can we detect inflationary NG via the 21-cm background?

Pillepich, Porciani & Matarrese, 2006;
→ use 3D analysis
Pillepich, Porciani & Matarrese, in prep.

see also Cooray 2006; Cooray et al. 2008

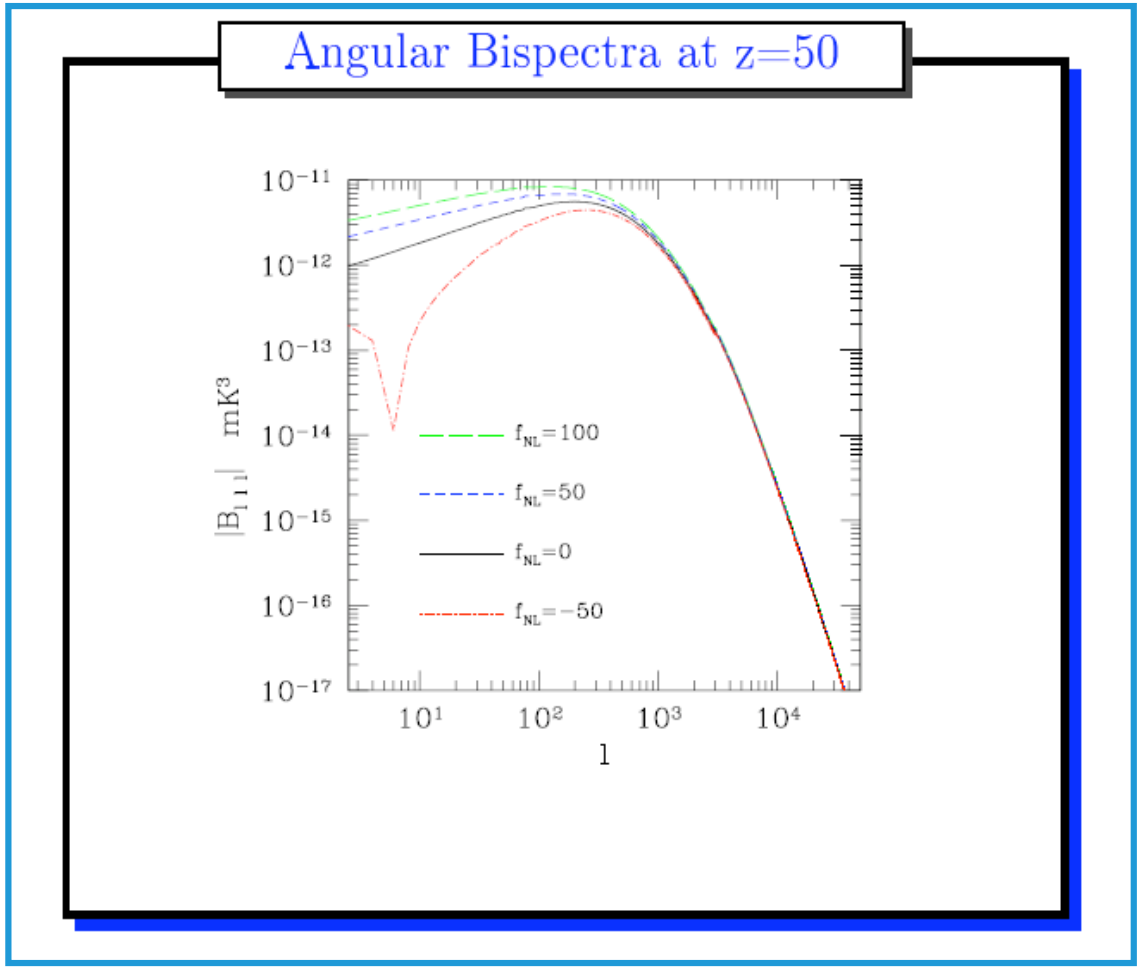

Is the expected NG signal detectable by future radio experiments?

Pillepich, Porciani & Matarrese 2006

Hypotheses:

- Ideal, full-sky experiment
- Measurements limited by cosmic variance only
- Perfect subtraction of foregrounds

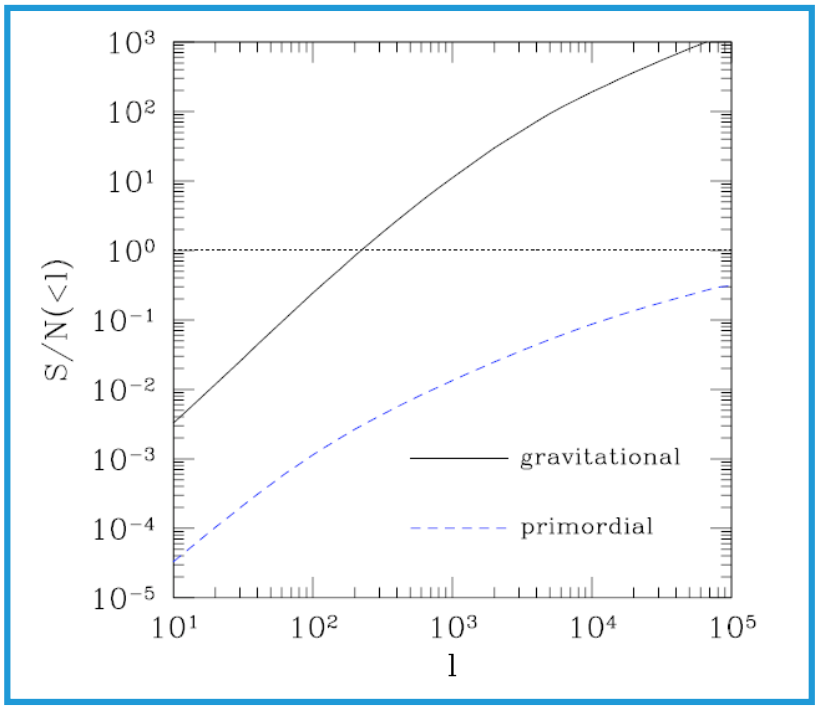

Warning: gravitational lensing can be very important!

Experiments with arcmin-scale resolution can measure →

- gravitational NG with S/N ~ 100
- primordial NG with S/N ~ 0.1 f_{NL}

Non-Gaussianities in the IGM

Viel, Dolag, Branchini, Grossi, Matarrese & Moscardini 2008, in prep.

Very first NG hydro simulations

NG initial conditions:

$$\Phi = \Phi_L + f_{NL}(\Phi_L^2 - \langle \Phi_L^2 \rangle)$$

$$\nabla^2(\Phi * T)g(z) = -4\pi G a^2 \delta\rho_{DM}$$

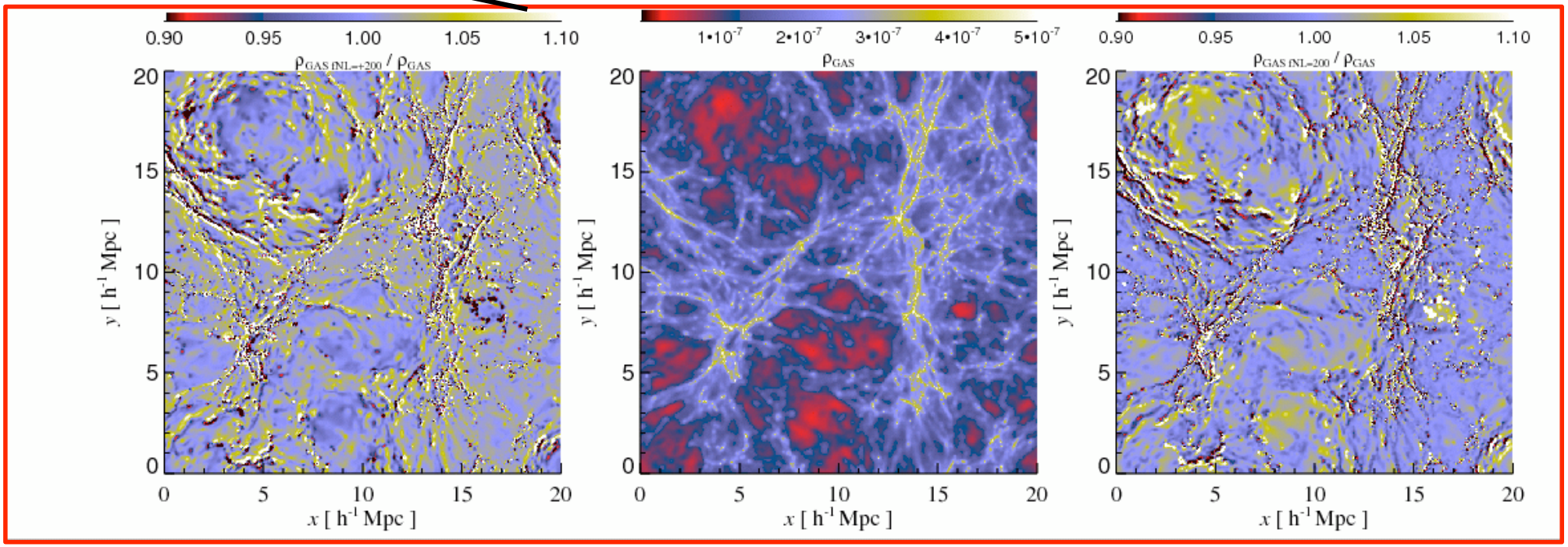

NG/G f_{NL} = 200 f_{NL} = 0 f_{NL} = - 200

GAS distribution in a slice of 3 Mpc/h (comoving) at z=3 (the voids have less and more matter compared to the standard case) – this in turn can be seen in the flux PDF

Non-Gaussianities in the IGM

Testing the PDF

DARK MATTER PDF

Grossi et al. 2008

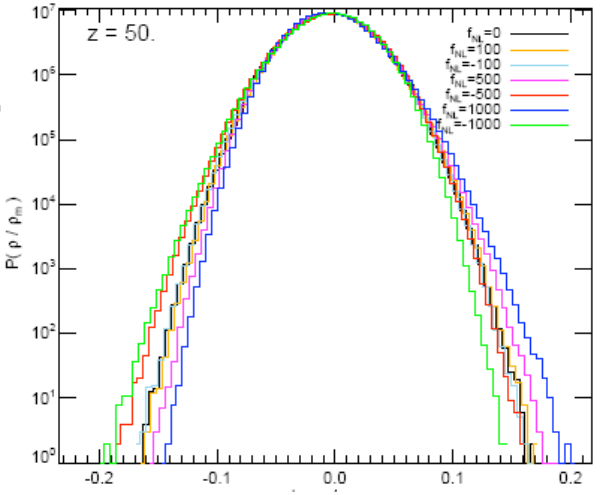

FLUX PDF (NG/G) Viel et al. 2008

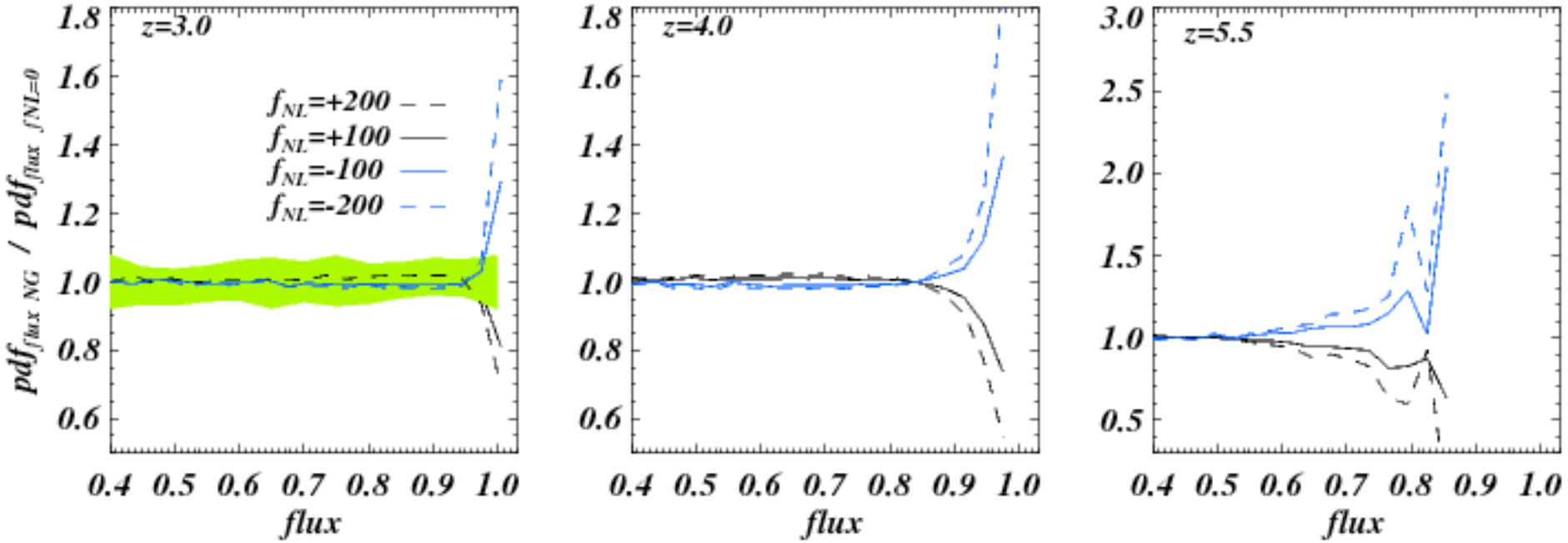

Viel, Dolag, Branchini, Grossi, Matarrese & Moscardini 2008, in prep.

FLUX POWER SPECTRUM

Statistical obs. error 0.6%

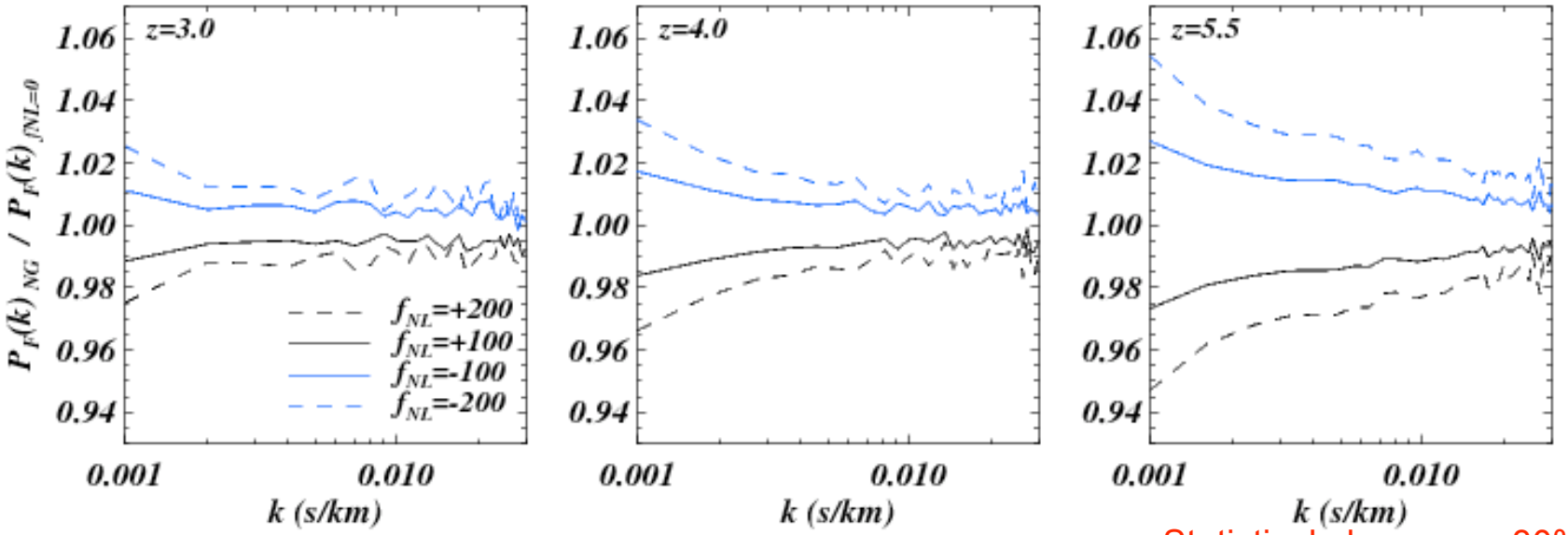

FLUX BISPECTRUM

Statistical obs. error ~30%

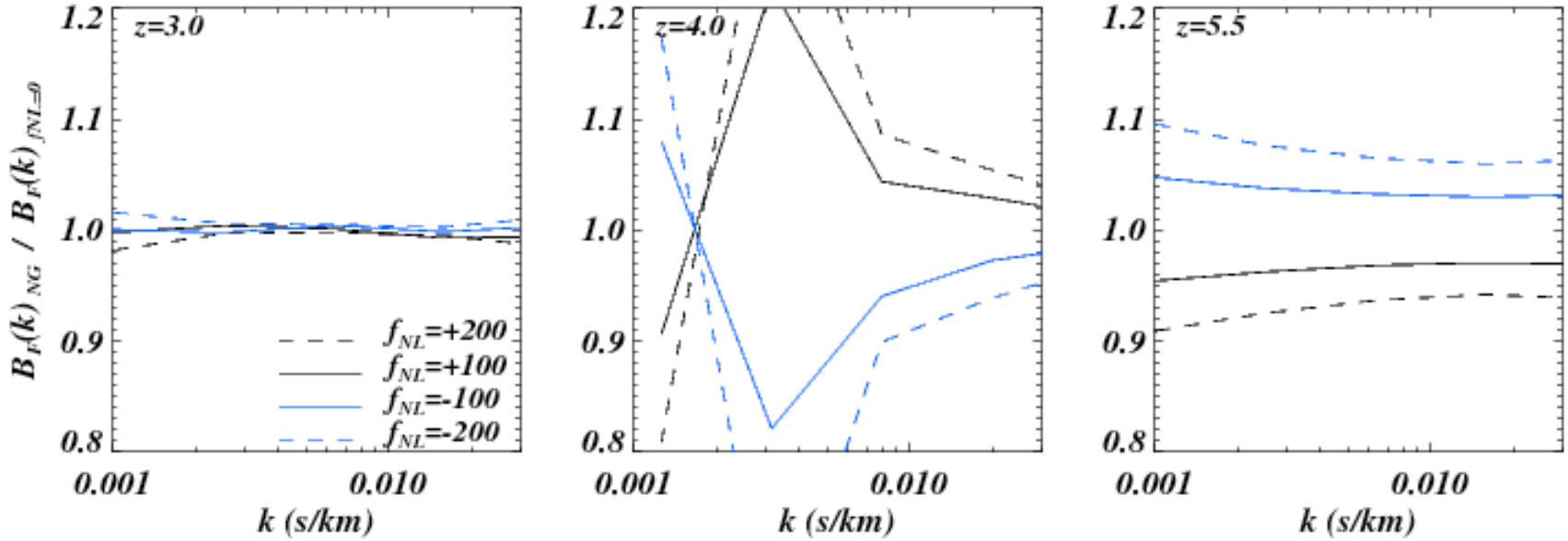

Flux bispectrum (Gaussian i.c.)

Viel, Matarrese, Heavens, Haehnelt, Kim, Springel & Hernquist 2004

Lots of astrophysical information in the high-redshift flux bispectrum

$$F = \exp\left[-A\,(1+\delta_{IGM})^{\beta}\right]$$

$$\delta_F \approx b_1[\delta^{(1)}(\mathbf{x}) + \delta^{(2)}(\mathbf{x})] + \frac{b_2}{2}\delta^{(1)\,2}(\mathbf{x}) \quad \text{with } b_1 = -A\,\beta \text{ and } b_2 = -A\,\beta\,(\beta - 1 - A\,\beta)$$

$$\begin{aligned} B(k_1,k_2,k_3) &= \left(\frac{12}{7}\,c_1 + c_2\right) p(k_1)\,p(k_2) \\ &+ c_1\left[(k_1\,k_2 - \frac{2}{7}k_1^2)\,p^{(-1)}(k_1)\,p(k_2)\right. \\ &+ (k_2\,k_1 - \frac{2}{7}k_2^2)\,p^{(-1)}(k_2)\,p(k_1) \\ &+ \left.\frac{6}{7}k_1^2\,k_2^2\,p^{(-1)}(k_1)p^{(-1)}(k_2)\right] + \text{cyc.}(1,2,3) \end{aligned}$$

where $c_1 = 1/b_1$, $c_2 = b_2/b_1^2$.

$$p^{(\ell)}(k) = |k|^{2\ell}\,p(k) + 2\,l\int_{|k|}^{\infty} dq\,q^{-2\ell-1}\,p(q)$$

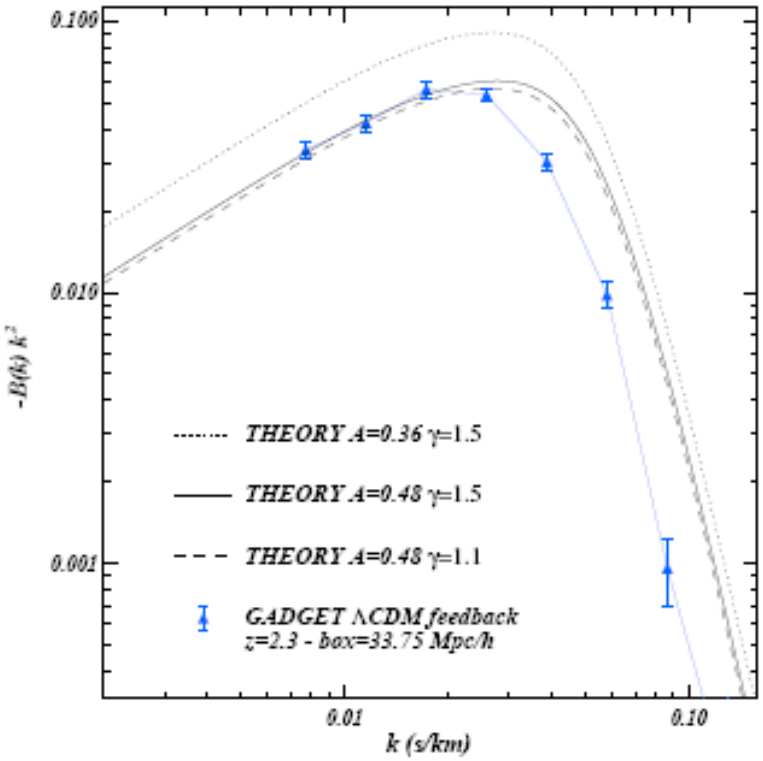

Conclusions & future prospects

- Contrary to earlier naive expectations, some level of non-Gaussianity is generically present in *all inflation models*. The level of non-Gaussianity predicted in the simplest (single-field, slow-roll) inflation is slightly below the minimum value detectable by *Planck* and at reach of future galaxy surveys.

- Constraining/detecting non-Gaussianity is a powerful tool to discriminate among competing scenarios for perturbation generation (*standard slow-roll inflation, curvaton, modulated-reheating, DBI, ghost inflation, multi-field, etc. …*) some of which imply large non-Gaussianity. Non-Gaussianity will soon become the *smoking-gun* for non-standard inflation models

- Constraining non-Gaussianity in LSS allows to put independent constraints on NG in a large range of scales: high-redshift samples (e.g. Ly-alpha forest, 21 cm background) appear promising. Using the galaxy bias is a powerful and promising technique, but … astrophysics should be under control!

- Predicting/constraining non-Gaussianity has become a branch of *Precision Cosmology.* The *Planck* mission (in combination with future galaxy surveys) will open a new window to the physics of the early Universe.